Process studies at the air-sea interface after atmospheric deposition in the Mediterranean Sea: objectives and strategy of the PEACETIME oceanographic campaign (May-June 2017)

Cécile Guieu[1], Fabrizio D'Ortenzio[1], François Dulac[2], Vincent Taillandier[1], Andrea Doglioli[3], Anne Petrenko[3], Stéphanie Barrillon[3], Marc Mallet[4], Pierre Nabat[4], Karine Desboeufs[5]

[1] CNRS, Sorbonne Université, Laboratoire d'Océanographie de Villefranche, UMR7093, Villefranche-sur-Mer, France

[2] Laboratoire des Sciences du Climat et de l'Environnement (LSCE), UMR 8212, CEA-CNRS-UVSQ, IPSL, Univ. Paris-Saclay, CEA Saclay, Gif-sur-Yvette

[3] Aix-Marseille Université, CNRS, Université de Toulon, IRD, Mediterranean Institute of Oceanography, UMR 7294, Marseille, France

[4] Centre National de Recherches Météorologiques, Météo-France/CNRM/GMGEC/MOSCA, Toulouse, France

[5] Laboratoire Interuniversitaire des Systèmes Atmosphériques (LISA), UMR CNRS 7583, Université de Paris, Université Paris Est Créteil, IPSL, Créteil, France

Abstract

In spring, the Mediterranean Sea, a well-stratified low nutrient low chlorophyll region, receives atmospheric deposition by both desert dust from the Sahara and airborne particles from anthropogenic sources. Such deposition translates into a supply of new nutrients and trace metals for the surface waters that likely impact biogeochemical cycles. However, the relative impacts of the processes involved are still far from being assessed in situ. After summarizing the knowledge on dust deposition and its impact on the Mediterranean Sea biogeochemistry, we present in this context the objectives and strategy of the PEACETIME project and cruise. Atmospheric and marine in situ observations and process studies have been conducted in contrasted areas encountering different atmospheric deposition context, including a dust deposition event that our dedicated 'Fast Action' strategy allowed us to catch. Process studies include also artificial dust seeding experiments conducted on board in large tanks for the first time in three ecoregions of the open waters of the Mediterranean Sea. This paper summarizes the work performed at sea and the type of data acquired in the atmosphere, at the air-sea interface and in the water column. An overview of the results presented in papers of this special issue (and in some others published elsewhere) is presented.

1. Introduction and rationale of the PEACETIME project

Understanding the exchange of energy, gases and particles at the ocean–atmosphere interface is critical for the development of robust predictions of future climate change and its consequences on marine ecosystems and the services they provide to society. Our understanding of such exchanges has advanced rapidly over the past decade but we remain unable to adequately parameterize fundamental controlling processes as identified in the new research strategies of the international Surface Ocean–Lower Atmosphere Study group (Law et al., 2013 and SOLAS 2015-2025: Science Plan and Organisation). A critical bottleneck is the parameterization and representation of the key processes brought into play by atmospheric deposition in Low Nutrient Low Chlorophyll (LNLC) regions. A perfect example of a LNLC region, and of the role of the atmospheric deposition, is the Mediterranean Sea where the ecosystem functioning may be modulated by pulsed atmospheric inputs in particular the deposition of Saharan dust (Guieu et al., 2014a) and nutrients of anthropogenic origin (Richon et al., 2018a, 2018b).

Indeed, the Mediterranean quasi-enclosed basin continuously receives anthropogenic aerosols originating from industrial and domestic activities from all around the basin and other parts of Europe, both in the western (Bergametti et al., 1989; Desboeufs et al., 2018) and eastern (Tsapakis et al., 2006; Moon et al., 2016) basins. In addition to these continuous 'background' inputs, the surface of the Mediterranean Sea episodically receives biomass burning particles (Guieu et al., 2005) and Saharan dust (e.g. Loÿe-Pilot et al., 1986, Vincent et al., 2016). Some deposition events are qualified as 'extreme events', as dust inputs as high as 22 g m^{-2} (event in Nov. 2001 recorded at Ostriconi-Corsica Island, Guieu et al., 2010; event in Feb. 2002 recorded at Cap Ferrat, Bonnet and Guieu, 2006) can occur on very short time scales (hours to days) representing the main annual dust flux. Associated atmospheric deposition of major macro-nutrient (N, P) (Kouvarakis et al., 2001; Markaki et al., 2003, 2010; Guieu et al., 2010), of iron (Bonnet and Guieu, 2006) and other trace metals (Theodesi et al., 2010; Guieu et al., 2010; Desboeufs et al., 2018) represents significant inputs likely supporting the primary production in surface waters especially during the stratification period (Richon et al., 2018a, 2018b). Among the atmospheric deposited nutrients, anthropogenic reactive nitrogen is critical on the fluxes of inorganic and organic N (Markaki et al., 2010, Violaki et al., 2010). Soil dust deposition plays an important role on the fluxes of P and trace metal due to the intense but sporadic inputs (Bergametti et al., 1992; Guieu et al., 2010; Morales-Baquero and Perez-Martinez, 2016), even if the contribution of anthropogenic aerosol deposition is significant (<10

% (Fe) up to 90% (Zn)) (Guieu et al., 2010, Desboeufs et al., 2018). The atmospheric deposition of mineral dust is correlated with dissolved trace metals enrichment of the sea-surface microlayer (Cd, Co, Cu, Fe) (Tovar-Sanchez et al., 2014). However, it has been shown that dust deposition can result either in a net release or in scavenging of dissolved inorganic phosphorus and nitrate (Louis et al., 2015) and trace elements in seawater (Wagener et al., 2010; Wuttig et al., 2013; Bressac & Guieu 2013), depending on the quantity and quality of in situ dissolved organic matter at the time of the deposition.

Recent studies in pelagic large mesocosms equipped with sediment traps, have shown that wet Saharan dust analog deposition, by providing P and N, strongly stimulates primary production and phytoplanktonic biomass during several days after the rain event was simulated (Ridame et al., 2014; Guieu et al., 2014b; Tsagaraki et al., 2017). In addition to being strongly stimulated by atmospheric P (Ridame et al., 2013), the trace metals in dust deposition have been also suspected to stimulate nitrogen fixation in the Mediterranean Sea (Ridame et al., 2011). The extension of this fertilizing effect of dust events over the Mediterranean has been pointed out from statistically positive correlations between dust deposition and surface chlorophyll concentrations from remote sensing and modelling approaches (Gallisai et al., 2014). A negative effect of atmospheric deposition on chlorophyll is, however, observed in the regions under a large influence of aerosols from European origin (Gallisai et al., 2014). Indeed, the input of anthropogenic aerosols, as Cu-rich aerosol, has been suspected to inhibit phytoplankton growth (Jordi et al., 2012). Besides phytoplankton, dust deposition modifies also the bacterial community structure by selectively stimulating and inhibiting certain members of the bacterial community (Pulido-Villena et al., 2014; Tsagarakis et al., 2017). The budgets established from 4 artificial seeding experiments during project DUNE (Guieu et al., 2014b) all showed that stimulating predominantly heterotrophic bacteria, atmospheric dust deposition can enhance the remineralization of dissolved organic carbon (DOC), thereby reducing net atmospheric CO_2 drawdown. This also reduces the fraction of DOC that can be mixed and exported to deep waters during the winter mixing (Pulido-Villena et al., 2008). Similarly, dust addition using on-land mesocosms in the eastern Mediterranean Sea suggested that the auto- and heterotrophic components of the food web were enhanced by the dust addition thanks to the nitrogen and phosphorus added through dust (Pitta et al., 2017 and companion papers). The response was independent of the way the dust was added to the surface waters (single strong pulse or three repetitive smaller pulses). One of the most intriguing results is the role of Saharan dust deposition in the export of particulate organic carbon (POC) to the deep Mediterranean Sea by

both fertilizing and acting as ballast and facilitating aggregation processes (i.e. Ternon et al. 2010, Bressac et al., 2014; Desboeufs et al., 2014; Louis et al., 2017). Experimental approaches have shown that wet dust deposition events, by supplying bioavailable new nutrients, presents a higher positive impact compared to dry deposition, on both marine primary production, nitrogen fixation and chlorophyll concentrations (Ridame et al., 2014; Guieu et al., 2014b). Over the past decade, most of these valuable findings have been made thanks to experimental approaches based on dust and aerosols addition into bottles and up to large in-situ mesocosms or using remote sensing approaches (Guieu and Ridame, 2020).

In this context, the PEACETIME project (ProcEss studies at the Air-sEa Interface after dust deposition in the MEditerranean sea) (http://peacetime-project.org/) aimed at studying and parameterizing the chain of processes occurring in the Mediterranean Sea after atmospheric Saharan dust deposition, and to put them in perspective of on-going environmental changes. The ultimate goal was to assess how these mechanisms impact, and will impact in the future, the functioning of the marine biogeochemical cycles, the pelagic ecosystem and the feedback to the atmosphere. The PEACETIME project was centered on a one-month oceanographic cruise in the central and western Mediterranean Sea in May-June 2017. The strategy during the cruise was designed to tackle the following questions:

1. How does atmospheric deposition impact trace element distribution in the water column including the sea surface microlayer?

2. What is the role of dissolved organic matter/particulate dynamics on the fate of deposited atmospheric trace elements?

3. How does atmospheric deposition impact biogeochemical processes and fluxes? Do in situ biogeochemical /physical conditions matter?

4. What is the impact of atmospheric deposition on biological activity and on the structure and composition of the planktonic communities?

5. How does atmospheric deposition impact the downward POC export and the subsequent carbon sequestration?

6. What is the impact of biogeochemical conditions on gases and aerosol emissions from the surface water?

7. How are optical properties above and below the air-sea interface impacted by aerosols emission and dust deposition?

During the 33-day cruise assembling 40 scientists from the atmosphere and ocean communities, the strategy was based on the sampling of a real dust deposition event with the characterisation of the chemical, biological, physical and optical properties of both the atmosphere and the sea-surface microlayer, mixed layer and deeper waters, before and after deposition. The time of the campaign and an adaptive strategy for the cruise track, based on the daily analysis of a number of operational forecast and near real-time observational products, were designed to maximize the probability of catching a Saharan dust deposition event in a stratified water column in order to follow in-situ the associated processes. Our strategy was successful since a wet Saharan dust event was indeed sampled during a dedicated period: the so-called "Fast action". However, this strategy was very dependent on the occurrence of a dust deposition event during the cruise, so to ensure results corresponding to our questions, simultaneous in situ sampling/characterisation in the lower atmosphere and the water column was performed on the route. This more classical strategy enabled also to investigate the impacts of air-sea exchanges on the cycles of chemical elements, on marine biogeochemical processes and fluxes, on marine aerosols emission in a variety of oligotrophic regimes. Moreover, on board dust seeding experiments were conducted in climate reactors simulating present and future marine physical conditions.

In this paper, we describe the strategy followed during the cruise with a focus on the adaptive strategy that permitted to study a wet dust deposition event at sea. We also provide a first overview of the results obtained.

2. Dust deposition and water stratification in Mediterranean Sea: best time to schedule PEACETIME cruise

In order to fulfill the objectives of the PEACETIME cruise, the occurrence probability of a significant atmospheric deposition event was maximized by choosing to do the cruise during a period of surface water stratification. This criterion matters because atmospheric inputs can be the main external nutrient supply to offshore surface waters during the stratification period (Guerzoni et al., 1999; The Mermex Group, 2011; Richon et al., 2018a). The Mediterranean surface mixed layer depth monthly climatology (Figure 1) shows a basin scale deepening from November to February–March and an abrupt re-stratification in April, which is maintained throughout summer and early autumn (D'Ortenzio et al., 2005). With mixed layer depths below 30 m in the whole Mediterranean basin, the May-September period looks particularly favorable to sample highly stratified waters.

Because African dust transport associated with the rainy period generally leads to the highest atmospheric deposition fluxes in the Mediterranean region (e.g., Loÿe-Pilot et al., 1986; Kubilay et al., 2000; Fu et al., 2017), we checked the probability that a Saharan dust event may occur during the cruise. The satellite-derived monthly climatology of dust in the atmospheric column over the Mediterranean show a maximum in summer in the western basin and in spring and summer in the central basin (e.g., Moulin et al., 1998; Varga et al., 2014). Consistently, model results in Figure 2 shows the highest values of dust aerosol optical depth (>0.10 and up to 0.30 at 550 nm) over the whole western and central basins from May to August, an intermediate situation in April and September, and the lowest values (generally <0.10) from October to February.

In addition to this seasonality of the dust columnar load, the climatology of particles with diameter smaller than 10 µm (PM10) and associated African dust concentration in the Mediterranean indicates that the occurrence of dust plumes close to the sea surface, i.e. prone to dry deposition, is maximum in April-May in Greece, April-June in Sicily, May-June in continental Italy, May in SE France, June-July in NE Spain and July-August in SE Spain (Pey et al., 2013). From weekly insoluble deposition monitoring at 4 sites of western Mediterranean islands (Frioul, Corsica, Mallorca and Lampedusa) in the period 2011-2013, Vincent et al. (2016) report that most of the most intense African dust deposition events (MIDD) occurred between March and June.

Literature from deposition measurements at various sites in the western Mediterranean highlights a spring maxima for dust deposition (Bergametti et al., 1989; Loÿe-Pilot and Martin, 1996; Avila et al., 1997; Ternon et al., 2010; Desboeufs et al., 2018). Moreover, observations indicate that the highest deposition fluxes of dust are most often associated with wet deposition episodes (e.g. Loÿe-Pilot et al., 1986; Bergametti et al., 1989; Guerzoni et al., 1995; Loÿe-Pilot and Martin, 1996; Avila et al., 1997; Kubilay et al., 2000, Dulac et al., 2004; Guieu et al., 2010; Ternon et al., 2010; Vincent et al., 2016). A survey of dust wet deposition events at Montseny stations in NE Spain over 1996-2002 concluded that the maximum frequency was in May (about three events per month) and June and November (about 1 event per month). Data from Vincent et al. (2016) also show that most of the two-three highest dust deposition events recorded at each of the four island stations cited above occurred between March and May, and are most often associated with rainfall.

It was also important that the cruise crossed different trophic regimes to get likely contrasted responses to atmospheric deposition. The central Mediterranean Sea (MS) was our main

targeted area since all the marine ecoregions of the MS can be found in a relatively small zone (Figure 1- Supp. Mat.). Although the Mediterranean is classified as an oligotrophic basin characterized by low-nutrient concentrations, there is a general west-to-east gradient of increasing oligotrophy (The Mermex Group (2011) and references within). Figure 3 shows monthly averaged satellite-derived Chl-a concentrations in the Mediterranean basin : from April to June, various trophic conditions can be found in the basin, with still relatively "high" Chl-a concentrations (0.3 mg m^{-3}) in the Ligurian and Alboran Sea and ultra-oligotrophic conditions in the central and eastern basin (< 0.03 mg m^{-3}) (Bosc et al., 2004).

From all the preceding considerations, we finally concluded that mid-April to mid-June was the target period for the cruise.

3. Implementation of the PEACETIME cruise

Based on the scientific arguments detailed above and on the availability of the ship, the PEACETIME cruise was conducted during late spring conditions from May 10 to June 11, 2017 on-board the French R/V Pourquoi Pas?

3.1 Transect of principle of the PEACETIME cruise

As shown in Figure 1- Supp. Mat., the initial transect designed for PEACETIME aimed at visiting most of the identified ecoregions within the 4 weeks of cruise, allowing us to test the impact of atmospheric deposition on a large range of natural assemblages. The planned long stations of the transect of principle were located within or at the center of three main ecoregions. Short stations (occupation time was less than 8 hours) were positioned in order that cruising between two stations was long enough (~8 hours) to allow the continuous measurement of both lower atmosphere and surface seawater while cruising. Depending on atmospheric conditions during the cruise, it was anticipated that one of the long stations (named FAST) would be dedicated to document a deposition event at sea, and that the forecasted occurrence of such an event would prompt a fast action plan that might lead to the change of the planned transect and ship route. It is important to note that a strong dust event occurred over the Tyrrhenian Sea while the R/V was leaving the port of departure (La Seyne s/mer) with no possibility to catch the event on time but that the interpretation of the results obtained in that region have to take into account this special feature (see details in Desboeufs et al., in prep., this issue, Bressac et al., in prep., this issue). Indeed, using particulate aluminium as a tracer of Saharan dust in the column water, Bressac et al. (in prep., this issue) calculated that the dust deposition have impacted several stations (St 4-St5-TYR-St6) with dust flux ranging from ~1.5 to 8 $g.m^{-2}$.

In the following sections, we first describe the work that was performed at sea and then present our adaptive strategy tools that allowed us to well position the stations according to in situ dynamic structures. It specifically allowed us to reroute the vessel 800 km (450 mn) away from the planned route to catch a dust event at the so-called FAST station (Figure 4).

3.2 Work at sea

All along the 4300 km transect (Figure 4), continuous monitoring of the lower atmosphere and the surface seawater was performed. In addition, the work at sea was divided between 10 short (~8 hours) and 3 long (TYR, ION and FAST, respectively 4 days, 4 days and 5 days duration) stations (Table 1). Between stations, the vessel was cruising at 9 knots providing at least 8 hours to perform a good continuous monitoring of both low atmosphere and surface waters while cruising. The total number of short stations allowed us to describe well enough stocks and fluxes along the whole water column and microstructure of the mixed layer in the contrasted biogeochemical regions crossed.

Long stations were located in 3 different ecoregions (Figure 1- Supp. Mat.) all characterized by oligotrophic conditions (see section 2). The duration of the long stations allowed processes studies both in situ (drifting mooring supporting different types of traps and instruments) and on-board (artificial dust seeding experiment in 300 L climate reactors).

Continuous and discrete characterisation of the atmosphere. Atmospheric sampling was carried out throughout the transect using PEGASUS dedicated mobile platform (PortablE Gas and Aerosol Sampling UnitS, Formenti et al., 2019) to monitor continuous air gaseous composition (NOx, SO_2, O_3, CO_2, CO, VOC), physico-chemical properties of aerosol particles (mass and number concentration, size-distribution, chemical composition and nutrients contents), parameters of atmospheric dynamics such as the boundary layer, and radiative parameters (incident radiation, optical thickness, optical properties of the particles). A specific device (Max-DOAS) dedicated to atmospheric halogen oxides measurements was also implemented during the cruise. Two rain events that occurred during the cruise have also been collected (29th of May and 5th of June) (see details in Desboeufs et al., in prep., this issue and Fu et al.(a), in prep., this issue). The on-line filtration collector was used to determine the dissolved and particulate composition of rain, including major and trace metals (Al, Ba, Cd, Co, Cr, Cu, Fe, Mo, Mn, Ni, Pb, Sr, Ti, V, Zn), atmospheric inorganic compounds (sulfate, chlorure, Na, Mg, K, Ca) and dissolved nutrients (phosphate, nitrate, ammonium).

Continuous and discrete characterisation of the surface waters and aerosols emissions. An innovative system of continuous "clean" pumping activated by a large peristaltic pump connected to a tube plunged at 5 m under the surface seawater inside a TravOcean was set up. The water was conveyed in a dedicated laboratory and distributed to several instruments to assess its chemical properties (carbonate chemistry, O_2), microbial assemblages, hydrological properties, optical properties related to particle composition and aerosol production (chemical composition, particles spectrum) throughout the transect. To study marine emission, the chemical composition of sea spray aerosols generated from the underway seawater system could be continuously measured online with an hourly resolution. A continuous water sampling is essential as it was recently shown that emissions have a diurnal variability that follows the biological activity (Long et al. 2014). Primarily produced particles were investigated for their size distribution, cloud condensation nuclei (CNN) properties, and chemical composition (filters).

Profiling while moving. A MVP (Moving Vessel Profiler) was deployed to perform high frequency 0-300 m profiles of CTD (and fluorescence and LOPC-Laser Optical Particle Counter, when the “big fish” was towed instead of the “small fish”) between the short stations and in the long station areas as frequently as possible. A total of more than 1000 profiles have been obtained.

Discrete sampling of the surface microlayer (SML). Sampling was performed from a rubber boat using gas plate systems. Dissolved (<0.22 µm) and total (unfiltered) SML samples were collected for trace metals (Cd, Co, Cu, Fe, Ni, Mo, V, Zn and Pb) and nutrients analysis. The same metals were also measured in a subsurface (0-1 m) filtered (0.22 µm) sample. Samples were collected for the determination of total combined carbohydrates, total hydrolysable amino acids, gel particles (TEP and CSP). DNA was extracted from filters from the surface microlayer and subsurface water (~ 20 cm). Three experimental SML additions were carried out in waters of TYR, ION and FAST stations.

Two types of rosette to depict the whole water column characteristics. The ”classical” Rosette was composed of a CTD underwater unit that continuously collected the following parameters: pressure, temperature and salinity of seawater, dissolved oxygen concentration, photosynthetically active radiation (PAR), beam transmission (at 650 nm), chlorophyll-a fluorescence. A LISST (Laser in situ Scattering and Transmissiometry Deep (LISST-Deep), Sequoia Sc) was mounted independently on the CTD frame. This instrumental package was also composed of a sampling system: 24 12-L Niskin bottles could be fired at specified levels

during upcasts. Some Niskin could be replaced by High Pressure (HP) bottles that allowed hyperbaric sampling on dedicated deep casts. Water from the classical Rosette was used to quantify O2, AT/CT, nutrients, DOC, POC/PON, hyperspectral particulate absorption coefficient, hyperspectral CDOM absorption coefficient, chlorophyll pigments, viruses abundance and lysogeny, bacteria, flagellates and pico-nanoeukaryotes abundance (by cytometry), total combined carbohydrates, total hydrolysable amino acids, gel particles (TEP and CSP), bacterial production, dissolved and particulate primary production, virus diversity, and eukaryote diversity. The trace metal "clean" Rosette was composed of a titanium CTD underwater unit that continuously collected the following parameters: pressure, temperature and salinity of seawater, dissolved oxygen concentration, CDOM Fluorescence. This instrumental package was also composed of a teflon-coated sampling system: 24 GoFlo bottles could be fired at specified levels during upcast. Water from the clean rosette was used to measure dissolved metals (Al, Cd, Co, Cu, Fe, Mo, Ni, Pb, V, Zn) and particulate (Al, Ba, Ca, Cu, Fe, Mn, Ni, Ti, Zn), total mercury, methyl mercury, inorganic phosphate and nitrate (nano-molar), nutrients (to be measured with Technicon), di-nitrogen fixation, diazotrophs diversity (only at Station 10). In addition, and at the daily solar maximum when the cloud cover permitted, the HyperPro instrument measured hyperspectral upwelling radiance (Lu) and downwelling irradiance (Ed).

Zooplankton abundance, biomass and taxonomy. Zooplankton samples were collected by net hauls between 0 and 300 m performed with a BONGO net equipped with a 100 µm and a 200 µm mesh size. Three size classes were considered: <200 µm; >200 - <1000 µm and >1000 µm. At long stations, additional zooplankton samples were taken for stable isotopes analyses.

3.3 Additional work at long duration stations.

Drifting mooring. A drifting mooring was equipped with (i) 3 Technicap type PPS5 particle traps at 200, 500 and 1000 m, each equipped with inclinometers, (ii) 3 IODA (In Situ Oxygen Dynamics Auto-analyzer) at 5, 90 and 200 m; (iii) 2 in situ particle interceptor/incubator – RESPIRE (at 120 m and 200 m), (iv) 2 trace metal clean RESPIRE (at 110 m and 190 m), and (v) 1 Sediment Trap Station with 4, ø80-mm tubes in transparent PVC. The line was also equipped with 4 CTD / O2 type SeaBird Microcat SBE37, 4 Aquadopp Doppler current meter from Nortek brand, 5 RBR Autonomous Temperature and Pressure Sensors, 5 RBR Autonomous Temperature Sensors alone. Drifting moorings were deployed for 4 days at TYR and ION and 5 days at FAST. Fluxes for particulate mass, carbon, organic carbon, inorganic carbon, nitrogen, calcium, aluminium, iron, biogenic and lithogenic silica were determined from PPS5 samples. At long duration stations a large "Marine Snow Catcher" bottle (100 L)

was also deployed to collect suspended particles, slow sinking particles and fast sinking particles. Heterotrophic production of prokaryotes attached to these different particle types was measured along with TEP abundance and POC concentrations. In addition, concentration kinetics of aminopeptidase, alkaline phosphatase and beta D glucosidase was measured. Diversity of microorganisms collected in each type of particles was analyzed by barcoding and sequencing. A total of 20 SVP (Surface Velocity Program) drifters were deployed at the long duration stations to provide information on the current at 15-m depth. Two Biogeochemical Argo profiling floats have been deployed in the Ionian Sea. In addition to the CTD, the floats interfaced bio-optical sensors that measured fluorescence of Chlorophyll and CDOM, particulate backscattering (700 nm), Photosynthetically Active Radiation and downwelling irradiance at three wavelengths (380, 412, 490 nm). In addition, the float released at the ION station included an optode that measures dissolved oxygen and a beam transmissometer (650 nm). Sediment core sampling was carried out with a multicorer, sliced into depth layers to perform DNA extractions at TYR (depth 3395 m), ION (depth 3054 m) and FAST (2775 m).

On-board perturbation experiments. Three perturbation experiments were conducted on board at each of the long duration stations. Inside a container, six "Climate Reactors" (volume of each tank = 300 L) were filled with surface water. After artificial dust seeding at the surface of 4 of the reactors, the impact of dust deposition on biogeochemical stocks and fluxes under present and future environmental conditions (acidification and increase of the temperature of the sea water) was followed during 4 days (TYR and ION) and 5 days (FAST). (40 parameters have been measured; see the full list in Gazeau et al., 2020].

Table 2 summarizes the operations conducted during the cruise and the parameters obtained, (1) on a continuous basis, (2) at short stations, and (3) at long stations and indicate the papers based on those results. An overview of the papers is presented section 6.

3.4 Tools for decision: the PEACETIME Operation Center

Based on the experience of the ChArMEx airborne campaigns (Mallet et al., 2016) and of previous oceanographic cruises needing an adaptive planning strategy based on observations and short-term forecasts, an operational server named the PEACETIME Operation Center (POC; http://poc.sedoo.fr/) was set-up by the Service de Données de l'Observatoire Midi-Pyrénées (OMP/SEDOO, Toulouse, France) for the cruise. It operated from early May to mid-June 2017, gathering a set of quick-looks of (i) near-real time selected remote sensing or other observational products and (ii) meteorological and chemistry-transport model forecasts, considered useful for the campaign planning decisions. Short- and middle-term forecast models

of weather conditions and of dust transport and deposition were systematically analyzed to verify the conditions, in order to eventually decide to start the Fast Action. The Fast Action strategy consisted in routing the ship towards an area of a forecasted dust deposition event in order to tentatively document the respective roles of dynamics and deposition on marine biogeochemical conditions. The goal was to position the ship in the center of the area of dust deposition, at least one day (24 hours) before the event in order to sample the water column before, during and after the deposition, and collect and characterize the rain event. In the Supp. Mat., more details are given on products that were found the most useful for daily decisions during the cruise. The quick-looks were either directly transferred to the POC following their production by respective operational centers, or linked from their original browser. Various reports were also produced and made available on a quasi-daily basis (this includes: meteorology and dust over the basin, regional and local oceanographic conditions, ship trajectory). The complete series of reports is available at http://poc.sedoo.fr/source/indexGarde.php?current=20170602&nav=Reports (last access 22 September 2020).

Concerning the oceanic conditions, several remote-sensing datasets were exploited using the SPASSO (Software Package for an Adaptive Satellite-based Sampling for Ocean campaigns https://spasso.mio.osupytheas.fr/; last access: 22 September 2020) in order to guide the cruise through a Lagrangian adaptive sampling-strategy with the aim of avoiding regions of complex circulation and dynamics (fronts, small scale eddies). The idea behind this approach was to aim at a situation where the air-sea exchanges dominate and lateral advection and diffusion can be neglected. Such an approach was already successfully adopted during several previous cruises such as LATEX (Nencioli et al., 2011; Doglioli et al., 2013, Petrenko et al., 2017), KEOPS2 (d'Ovidio et al., 2015), OUTPACE (Moutin et al., 2017; de Verneil et al., 2018) and OSCAHR (Rousselet et al., 2019). During PEACETIME, we used the following datasets: (1) altimetry data from the AVISO Mediterranean regional product (https://www.aviso.altimetry.fr/data/products/sea-surface-height-products/regional/mediterranean-sea-gridded-sea-level-heights-and-derived-variables.html); the altimetry-derived currents were then processed by SPASSO to derive Eulerian and Lagrangian diagnostics of ocean circulation: Okubo-Weiss parameter, particle retention time and advection, Finite Size Lyapunov Exponent (e.g Figure SI-2); (2) the sea surface temperature (level 3 with resolutions of 4 and 1 km) and (3) the chlorophyll concentration (level 3 with a resolution of 1 km, MODIS Aqua and NPPVIIRS sensors combined after May 27, 2017 into a

unique product) provided by CMEMS - Copernicus Marine Environment Monitoring Service (http://marine.copernicus.eu/).

All these elements were simultaneously analysed during a daily meeting between scientists involved on land and on ship, as well as with the crew. Each day, the initial plan was confirmed for the next 48 h or, eventually, modified. For the first half of the cruise (Figure 4), only slight modifications of the initial plan were decided, as atmospheric conditions were not considered favorable for the Fast Action. They dramatically changed on the 28th of May, during the sampling of the ION station, leading to the decision to start the Fast Action which involved to move some 800 km (450 nm) from the position where the boat was located.

4. The decision process to start a FAST action and description of the Saharan dust event

On the 28th of May, a low pressure system reaching Spain from the Atlantic, a typical situation for African dust transport in summer in this area (Moulin et al., 1998) caused a southern flux over the western basin. At the end of station 8 on 30th May, satellite observations showed the presence of atmospheric dust in a cloudy air mass over the western part of the Mediterranean and long-term predictions of AOD indicated the continuing presence of dust over the Alboran Sea, with a new dust plume likely extending northwest on June 2 or 3. Although meteorological models diverged in forecasting rain over this region, the southwestern part of the Mediterranean basin looked to be the most dusty area for the next days and it was decided to modify the initial plan and to move towards the west for the last part of the cruise (see figure 4, the long transect in red). On May 31st, the ship reached a position approximately located between the islands of Sicily and Sardinia. Significant dust emissions were again observed over North Africa from the night of 30-31 May on, and the predictions for a new significant dust event over the southwestern Mediterranean on June 3-5 were confirmed. Although the differences between the models were still important (only SKIRON forecasted a wet deposition event south of Spain for the 3-4th of June), it was decided to continuously move the ship 800 km westward, and to shift station 9 from its initial position in the Tyrrhenian Sea to a new position in the Alboran Sea. We considered that establishing the area of next operations in the Alboran Sea could facilitate the re-positioning of the ship in the case of a confirmed prediction of a wet deposition event.

On the 1st of June, during the sampling at station 9 midway between Sicily and Spain, it was decided to start the Fast Action. Indeed, dust emissions continued in Algeria and southern Morocco associated to a southern flux, aerosol transport models confirmed a new significant

dust episode with AOD >0.8 (i.e. roughly 1 g m^{-2} of dust in the atmospheric column) for June 3-5, and the occurrence of associated rains appeared most likely from most meteorological forecasts. SKIRON and NMMB-BSC predicted the dust wet deposition flux to be more important on 3rd of June in the Alboran Sea west of 0° longitude, of the order of 1.5 and 0.5 g m^{-2}, respectively), but longer-term forecasts by SKIRON predicted wet dust deposition more east south of the Balearic Islands on June 4 (~0.5 g m^{-2}) and especially during the first half of June 5th (possibly >1.5 g m^{-2}), a possibility confirmed by other rain forecasts. The Fast Action station was positioned 145 km south the Balearic Island of Mallorca and 126 km north of the Algerian coast (Figure 4), where a limited portion of the sea is part of international waters (i.e. not included in an EEZ), and in an area where the influence of Atlantic waters characterized by different nutrients pattern than Mediterranean waters should be limited compared to the more western Alboran Sea. The ship reached the FAST station location on June 2 at the end of the day (Table 1) and the ocean and atmospheric sampling started immediately. The SEVIRI AOD remote sensing confirmed the export of a dust plume from North Africa south of the Balearic Islands with high AOD (>0.8; Figure 6) and NASCube confirmed new dust emissions in the night from 3 to 4 June. The dust plume was transported to the NE up to Sardinia on June 4, with AOD <0.5 in all the area and clear sky with low AOD was left west of 4°E on June 5 (Desboeufs et al., in prep., this issue). In the same time, a rain front, moving eastward from Spain and North Africa regions, reached the Fast Action position the night between June 4 and 5 (Figure 5).

A single intense rain event was observed and sampled on board at the station FAST on June 5 from 2:36 am to 3:04 am. This rain was part of a massive rain front covering ~80 000 km^2. This front extended from the coast of Spain to the south of the FAST station area, with rain rate reaching 10 mm h^{-1} (Figure 5). Continuous lidar measurements on board the ship confirmed the presence of a dust layer mainly over the atmospheric boundary layer over the FAST station and its below-cloud deposition during the rain event of early June 5 (Desboeufs et al., in prep., this issue). The chemical composition of this rain confirmed a wet deposition dust event reaching a total particulate flux of 12 mg m^{-2} (Fu et al. (a), in preparation, this issue), which is in the low range of most intense dust deposition (MIDD) fluxes recorded in this area from long time-series of deposition network (Vincent et al., 2016). Using the time evolution of particulate Al stock in the upper 20 m before and after the event along with the lithogenic material flux collected by sediment traps, Bressac et al. calculated that the dust flux was much higher, of the order of ~65 $mg.m^{-2}$. The discrepancy between estimation from one single rain collected on board compared to integration of the dust deposition in the upper column water is quite logical as the rains were

patchy over the zone and a single sample certainly cannot be representative of the several events that took place over the whole area. Wet deposition of dust for June 4 and early June 5 over the FAST station area were also confirmed by the deposition maps from the 3 regional dust transport model forecast runs of June 2, with large differences in between models, from a very small flux of a few mg m^{-2} (BSC-DREAM8b) to about 100 mg m^{-2} (NMMB-BSC) and up to more than 1 g m^{-2} (SKIRON) (Figure Supp. Mat. 5).

5. Overview of marine conditions during the cruise

5.1 General oceanic environmental pattern along the cruise track

In figure 7, we show the satellite-derived SST data averaged taking into account the ship position. During the cruise, a general warming of the sea surface was observed and the FAST station has been performed in waters warmer than the two others LD stations.

Chlorophyll concentrations as seen by satellite over the western and central Mediterranean Sea were typical of the oligotrophic conditions encountered during the season characterized by a strong stratification (Figure 8). The west-east gradient between oligotrophic to very oligotrophic was clearly established and minimal concentrations (about 0.05 mg m^{-3}) were observed in the Ionian Sea.

Surface inorganic nutrients measured at nanomolar concentrations were very low for both dissolved inorganic nitrogen (DIN) and phosphorus (DIP). Indeed, average concentration in 0-20 m layer was 90 nM DIN and 15 nM DIP at the westernmost station (station 10) and 14 nM DIN and 10 nM DIP at the easternmost station (ION). Along the longitudinal transect, a deepening of the nutrient depleted layer toward the east was observed (figure 9) consistent with the general trend of those nutrients in the Mediterranean basin as described in Mermex Group (2011) and references inside.

5.2 Specific features of the FAST station

Sea Surface dynamic context. Several approaches have been implemented to highlight the dynamical context around the FAST station in the waters above 200 m, the physical structures and the possible influences of the dynamics on the stability of the water masses at the station. These approaches are based on in situ observations (Moving Vessel Profiler (MVP) transect and drifters trajectories) and diagnostic tools. On board, a MVP collected high frequency Conductivity- Temperature- Depth (CTD) data along two transects: the first one when the vessel approached the FAST station from the east, before the station took place, and the second

one west of the FAST station (back from the westernmost station 10) 7 days after the first transect. Figure 10 shows these data in a longitude-depth section.

To the east of the FAST station, the surface water was colder than to the west, likely due to synoptic cooling of the surface that occurred in the time interval between the two transects. Density section shows a strong deformation of the isopycnals west of the station FAST, which suggests the presence of an anticyclonic eddy (Taupier-Letage et al., 2003). It was characterized by a low salinity core from the surface down to 200m, carrying recently modified Atlantic waters. The map of the altimetry derived currents shows the presence of the mesoscale eddy west to the FAST station, confirmed by the inversion of VM-ADCP currents collected across the western transect (Figure 11). According to these satellite and in-situ currents, the eddy is centered around (37°30'N, 1°40'E) where the surface current is reversed, its extension reaches the 2°30'E meridian, which leads to a radius of about 60 km.

SVP drifters have been deployed around the FAST station between 2°30'E and 3°15'E. Their trajectories showed a slow surface motion around the station, then SSW drifts heading 220° similar for all the buoys (figure 11). The observed trajectories have been accurately reproduced by numerical particles dispersed inside the altimetric derived surface currents that account for the Ekman drift calculated with wind data from the high resolution regional model WRF 3.7. This also allowed to calculate backward trajectories of the surface water masses using the ARIANE Lagrangian tool (Blanke and Raynaud, 1997; Blanke et al., 1999) in order to estimate the origins of the sampled surface water at the FAST station. Over the whole station duration, a mean value of 57 and 26 % of water remained in the station zone after 1 and 2 day(s), respectively. Moreover, combining the particle trajectories and the precipitation data from the WRF 3.7 model, the rainfall, which occurred slightly upstream the FAST station in the previous days, likely impacted the sampled water mass (Figure 12).

Temporal evolution of surface seawater properties during FAST. FAST station has been documented at its fixed point during 5 (+1) days by 43 repeated CTD casts in the depth range 0-200 m. The hydrological situation was characterized by a very shallow surface mixed layer and a sharp seasonal thermocline that extended underneath down to 75 m depth (Figure 13, upper right and middle right panels). In this upper layer, salinity values were lower than 37.5, which is characteristic of modified Atlantic waters flowing eastward inside the Mediterranean Sea. In the deeper layers, salinity increased sharply with depth until 350 m where it reached its maximum value (38.59), which is characteristic of Levantine intermediate waters flowing westward into the Mediterranean outflow. Deep waters, formed at winter convection zones of

the northwestern Mediterranean, had lower salinity values (38.48); they extended from 1400 m down to the sea bottom. The hydrological conditions at this site between June 2 and 8 during the Fast Action mainly evolved in the upper layer (Figure 13, upper left and middle left panels). The surface mixed layer was shallow with variations from 9-m to 19-m depth following the diurnal cycle. Mixed layer salinity remained equal until June 7; in particular no dilution effect due to the rainfall on June 3 and 5 has been recorded. The stratification of the whole water column remained steady during the long station. The density horizons being maintained along isobars in the upper layer, sign the absence of geostrophic perturbations during the long station. However, the current profilers indicated a depth-independent (barotropic) motion of amplitude 3 cm s^{-1} heading 220°, which is in agreement with the position of the station within the large eastern Algerian Gyre, a component of the basin scale cyclonic circulation described by Testor et al. (2005). This southwestward flow transported superficial water masses of distinct properties as clearly marked below the mixed layer by salinity anomalies (referenced to the initial profile of 2nd June 16:30). These water masses crossed the observation site, disrupting the water column in the depth range of 25-100 m, lowering salinity values by 0.1 in the extension of the thermocline and increasing salinity values by 0.05 underneath. Although clearly present, this hydrological anomaly did not affect the surface waters and the MLD was stable during the Fast Action precluding any input from below that could have been linked to destratification induced by strong wind associated to the dust event (Desboeufs et al., in prep. this issue) as hypothesized in Guieu et al. (2010) from time-series observations in the northwestern Mediterranean Sea. Such conditions are favorable to observe any change strictly attributed to external inputs from above (i.e. atmospheric deposition).

The distribution of phytoplanktonic biomass has been detected by optical sensors mounted in the CTD package (Figure 13 lower panels): measurements of fluorescence and of beam transmission provided similar patterns, stressing the biogenic character of particles present in the water column. Intermittent signals at the sea surface has been detected only by transmissometry, however no clear relationship with the rain event can be stated (see the first profile after event in red). A deep chlorophyll maximum of about 20-m thickness was located at the base of the thermocline (about 75 m). Short-term evolution during the 5 days of observation displayed variations in intensity and depth of the deep chlorophyll maximum, as well as splitting and merging sequences of the peak. Such perturbations appeared after the rain event of June 3, however they more likely result from the intrusion of water masses from north at this depth range. This hypothesis is reinforced by the absence of any geostrophic perturbation

in the density time series that could have injected biomass or nutrients via diapycnal processes. Another candidate could be the mixing effect associated to the breaking of internal gravity waves that propagated along the thermocline.

6. General overview of the papers resulting from the cruise

The PEACETIME cruise offered the opportunity to study along the 4300 km travelled both the lower atmosphere and the water column in contrasted biogeochemical regions of the Mediterranean Sea under the influence of different air masses and submitted to contrasted atmospheric deposition.

6.1 Atmosphere, surface microlayer and emissions back to the atmosphere.

Continuous atmospheric measurements allowed us to document the composition of the lower troposphere in contrasted areas from the remote Ionian Sea to Balearics Islands through the Tyrrhenian Sea and Messina Strait characterized by a high maritime ship traffic (Desboeufs et al, in prep.**,** this issue). Local wind and air masses trajectories analysis showed the influence of distinct air masses (from eastern and western Europe, as well as from Sahara), and various levels of concentrations, enabling to characterize background, polluted or dusty atmospheric conditions. The background level of the most common atmospheric pollutants for Mediterranean open-sea were quantified and discussed in terms of atmospheric reactivity (Desboeufs et al., in prep., this issue). Both bromine oxide (BrO) and iodine oxides (IO) have been modelled to be present in the Mediterranean marine atmosphere, however their detection has not been demonstrated yet. The first observations of the widespread presence of BrO and IO were reported over the Mediterranean atmosphere. These levels of halogen oxides can cause considerable impacts on the overall tropospheric ozone budget over the Mediterranean and affect pollutant and oxidant levels in Mediterranean coastal cities **(**Garcia-Nieto et al., pers. com.**).** Particulate and dissolved fractions of two wet deposition events collected on board, - one of which being the dust wet deposition at the FAST station - have been characterized (Fu et al. (a), in prep., this issue). Wet and dry atmospheric fluxes of nutrients and bioactive trace metals to the surface waters were derived from aerosols and rain concentrations measurements. The highest fluxes were found for the wet deposition event at FAST. Trace metals fluxes both from dry and wet depositions were significantly lower than those reported in the literature at coastal sites, emphasizing the relevance of offshore measurements to accurately quantify actual atmospheric inputs to the open ocean (Fu et al., a and b, in prep. this issue). Anthropogenic signature of aerosols chemical composition, in particular for trace metals, was obvious even in

the most remote areas, showing a clear anthropogenic influence in the Mediterranean background **(**Fu et al. (b), in prep., this issue**).** In agreement with GEOTRACES protocol, Fu et al. (pers. com) used a sequential two-stage leach to investigate the variability of fractional solubility of a suite of trace elements in aerosols (Al, Cd, Co, Cr, Cu, Fe, Mn, Mo, Nd, Ni, P, Pb, Ti, V), that was found directly related to the anthropogenic signature of aerosols. The soluble dry deposition fluxes were also determined. During the PEACETIME cruise, a special focus was also on the ship-plume contribution to atmospheric aerosols composition and deposition. The impact of marine traffic on aerosols composition, in particular for organic matter, was studied both when the instruments were directly under the influence of the R/V plume and while cruising in the Strait of Messina (a major navigation route connecting the West and East Mediterranean). Source apportionment allowed to determine a shipping organic aerosol factor, similar to the Hydrocarbon-like Organic Aerosol (HOA) factor, classically observed at urban sites from vehicular exhaust emissions, which could be useful to discriminate this source in atmospheric deposition measurements (Riffault et al., pers. com).

Thanks to discrete sampling of the SML away from the R/V, the interface between the atmosphere and the ocean has been shown to accumulate eukaryotic and prokaryotic micro-organisms (Zanker et al., 2020**)**. Even though decreasing abundances of phytoplankton and bacteria within the SML suggest that conditions become more hostile for microbes going from west to east in the Mediterranean Sea, semi-labile organic matter such as microgels and total carbohydrate are still present in the surface. While the neuston diversity might be decreasing, selecting for more oligotrophy-adapted protists, certain species might still be able to thrive, such as the fungi in the surface of the Ionian Sea (Zanker et al., 2020). A rapid increase of gel particles abundance in the SML was observed at station FAST directly after the dust deposition event, indicating a potential influence of atmospheric processes on organic matter dynamics at the air-sea interface (Engel et al. pers.com). SML was also shown to be very important for the exchange of some metals from aerosols which residence time within the surface microlayer were very different among chemical elements (in the order of minutes for iron up to several hours for copper) (Tovar-Sanchez et al., 2020)**.** The highest concentrations of trace metals (and bacteria) in the SML were observed after the dusty rain in the FAST station. The total concentrations of some reactive metals (i.e. Cu, Fe, Pb and Zn) were positively correlated with bacterial abundance, following the same decreasing eastward trend. This likely indicates that bacterioneuston plays a key role in controlling the concentrations and fates of those metals in the SML (Tovar-Sanchez et al., 2020). Interestingly, a strong negative correlation was found

between Ni concentration and heterotrophic bacterial abundance in the SML, along the whole transect that could be linked to a toxicity effect.

The emission of aerosols from the ocean to the atmosphere was also a focus of the PEACETIME project. During the cruise, Freney et al. (2020) have shown that the composition of sea spray reflected the oligotrophic conditions encountered along the transect, with an average 22±6 % organic matter content. Although this low content had little variations throughout the transect, it was mostly correlated with the particulate organic carbon seawater concentration and could be predicted using this variable. Moreover, the organic content of sea spray aerosols could be discriminated into several organic classes, each of them having specific climate-relevant properties. For instance, the Mixed Organic Aerosol (MOA) class, especially linked to the nanophytoplankton cell abundance, has an impact on the seawater surface tension, that in turn determines the number of sea spray particles and cloud condensation nuclei emitted to the atmosphere (Sellegri et al. in rev.). Neither the chemical composition, nor the number emissions of sea spray and cloud condensation nuclei were significantly influenced by the occurrence of the dust rain event during the FAST action. Neither was the ice nucleating ability of sea spray, although the ice nucleating ability of the SML was significantly enhanced (Trueblood et al., 2020), in relation with the enrichment of iron and bacteria cell number in the SML during this event.

6.2 Biogeochemical and physical features from instruments

Below the sea surface, a number of observations acquired with instruments deployed during the cruise (see Table 2) or thanks to autonomous floats launched well before and during the campaign, allowed to depict interesting features regarding transport of particles by water masses, nutrients dynamics and biological production. A high resolution quantification of particulate matter distribution by LOPC-Laser Optical Particle Counter, revealed potential long distance transport in the central Ionian Sea, bringing together particulate matter originating from the Northern Ionian and Modified Atlantic water masses (Berline et al., in prep this study**).** The role played by vertical diffusion in the nutrient enrichment of the Levantine Intermediate Waters was assessed (Taillandier et al., 2020), this process being particularly relevant inside thermohaline staircases. Thanks to a high profiling frequency over a four-year period, BGC-Argo float observations revealed the temporal continuity of the layering patterns encountered during the cruise PEACETIME, and their impact on vertical and lateral transfers of nitrate between the deep reservoir and the surface productive zone (Taillandier et al., 2020). From the diel cycles of optical properties measured by BGC-Argo profiling floats in the entire water

column, it was possible to derive estimates of biological production **(**Barbieux et al., in prep, this issue), revealing that the subsurface chlorophyll maximum (SCM) contributed substantially (~ 40%) to the biological production of the whole productive layer during the summer period in the Ligurian Sea. In the Ionian Sea, the SCM contributed less importantly to the summer time production than in the Ligurian Sea, but still in a non-negligible way (~ 20%). Hence, Barbieux et al. work suggests that because the SCM layer may contribute substantially to the total production of the water column in Mediterranean oligotrophic waters, it may be missed by estimates derived from ocean color satellite surface chlorophyll a data.

6.3. Biogeochemistry from discrete sampling during PEACETIME

The vertical distribution of chlorophyll, phytoplankton carbon biomass and primary production, together with bacterial production, with a focus on the deep chlorophyll maximum (DCM) was established along the cruise track (Marañón et al., 2020)**.** The DCM was also a primary production maximum, with an enhanced contribution by diatoms, which sustained similar biomass turnover rates to those found in well-lit surface waters. Bacterial production tended to peak at the surface and at or above the DCM, and bacterial carbon demand exceeded dissolved primary production. Among primary producers, a focus has been placed on diazotrophs (Ridame et al., in prep. this issue). The depth-integrated (0-100 m) di-nitrogen fixation rates encountered a low spatial variability between the different Mediterranean basins, except at station 10, in the Algerian basin where the fluxes were unusually high for the Mediterranean Sea (up to 72 nmol N. L^{-1}. d^{-1} at 60 m). At that station, the diazotrophic community was dominated by UCYN-A that represented more than 90% of the nifH population (Ridame et al., in prep. this issue). Specific phylotypes partitioned with depth layers with UCYN-A1 being the most abundant in surface water (<10 m) and with the relative abundance of UCYN-A4 increasing with depth (from 60-90 m), while a mix of the different phylotypes was observed at 200m. Ectoenzymatic activities (alkaline phosphatase, aminopeptidase and b-glucosidase) were determined for high and low affinity enzymatic systems at four selected layers (surface, deep chlorophyll maximum, LIW core and upper mesopelagic layer) (van Wambeke et al., 2020). The in situ aminopeptidase hydrolysis rates of dissolved N-proteins represented about 48% of the heterotrophic bacterial N demand in epipelagic layers (van Wambeke et al., 2020). Within the surface mixed layer, the contribution of this N source to N demand of heterotrophic bacteria was on average 1.4 times higher than total (organic + inorganic) dry atmospheric deposition determined at the same time (van Wambeke et al., in prep. this issue). Cross-basin simultaneous measurements of nanomolar phosphate concentrations, atmospheric deposition and alkaline

phosphatase activity are presented in Pulido-Villena et al., in prep, this issue. For the first time, the relative contribution of diapycnal fluxes and atmospheric inputs to phosphate supply to surface waters is assessed and compared to phosphate supplied by hydrolysis of organic phosphorus to satisfy P requirements. Diapycnal flux of phosphate to the mixed layer was particularly weak at FAST and was 2 order of magnitude lower than atmospheric soluble flux (Pulido-Villena et al., in prep). Vertical diffusion fluxes from the interior into the depleted layer (across nutriclines) were much higher (Taillandier et al., 2020, Pulido-Villena et al., in prep); however, those nutrients were not injected up to the shallower mixed layer that was rather directly impacted by atmospheric deposition as depicted at ION and FAST after wet deposition (van Wambeke et al., in prep., this issue). Thanks to a high frequency sampling and measurements of nutrients at nanomolar level, the rapid and short impact of those rains on the dynamics of N and P biogeochemical cycles and biological activity were investigated (van Wambeke et al., in prep., this issue).

By studying the zooplankton taxa assemblages in the Tyrrhenian Basin few days after a dust event and at FAST before and after a dust event, PEACETIME offered the first in situ observation of mesozooplankton responses to natural Saharan dust depositions **(**Feliu et al., 2020). The changes in mesozooplankton taxonomic structure appear to be a relevant indicator of that response, with an initial phase with no real dominance of taxa, then a disturbed state of the community with strong dominance of certain herbivorous taxa and the appearance of carnivorous species, and finally a recovery state towards a more stable system with diversification of the community (Feliu et al., 2020).

6.4 Mesopelagic processes

Simultaneous measurements of dissolved and (suspended) particulate concentrations, along with the sinking fraction (PPS5 sediment traps), were used to estimate the residence time of Aluminium and Iron at the three long stations submitted to contrasted atmospheric deposition conditions (Bressac et al., in prep., this issue). This study confirms the important dust deposition that affected a large area few days before our arrival in the Tyrrhenian Sea. Results are discussed and related to the origin (Saharan vs. anthropogenic), magnitude (2 to 3 orders of magnitude difference), and timing (few days before vs. during the occupation) of the atmospheric deposition events. At the FAST long station, the sampling performed at a high temporal/vertical resolution during a wet dust deposition event allowed estimating *in situ* the Fe and Al dissolution rates and the magnitude of post-depositional processes (e.g. scavenging) (Bressac et al., in prep., this issue).

Bressac et al. (2019) compared concurrent oxygen consumption, DFe and Fe-binding ligand replenishment rates in the Mediterranean Sea (PEACETIME) and Southern Ocean (EDDY, SOTS), two contrasting biogeochemical provinces characterized by differing contributions from biogenic and lithogenic sinking material. Mesopelagic iron regeneration efficiencies were heavily influenced by particle composition with 10- to 100-fold higher values in low-dust subantarctic waters relative to high-dust Mediterranean sites. Such wide-ranging regeneration efficiencies drive different vertical patterns in DFe replenishment across oceanic provinces. Further analyses by Whitby et al. (2020) demonstrated the importance of eHS in supporting DFe supplied by particle degradation, and highlighted how microbial removal of eHS ligands with increasing POC consumption could influence the amount of DFe resupplied by bacterial remineralization.

Particulate biogenic barium (Baxs) in the mesopelagic layer (100-1000 m depth) formed during organic matter degradation by heterotrophic prokaryotes, was used as a proxy for particulate organic carbon (POC) remineralization (Jacquet et al., submitted). Important spatial variability in POC remineralisation was measured, being for example more important and deeper in Algeria and the Ionian Basin compared to the Tyrrhenian Basin. Higher lithogenic impact on Ba signal (>20%) was found at Stations 4, 5 and TYR (250-450m) (based on Al correction) and could be related to the strong dust event that occurred few days before our arrival (see section 3.1 and Desboeufs et al., in prep this issue).

6.5. Present and future impact of dust deposition: results from on-board experiments.

The impact of dust deposition both in present and future climate conditions was assessed through perturbation experiments performed for the first time in the open Mediterranean Sea during the PEACETIME cruise. Experiments were conducted in large Climate reactors (300 L) at the long stations to test the impact of dust deposition on biogeochemistry stocks and processes and compare those impacts in contrasted open waters. Both temperature and pH were considered in order to test the effects both under present and future climate conditions. The experimental protocol comprised two unmodified control tanks, two tanks enriched with a Saharan dust analog and two tanks enriched with the dust analog and maintained under warmer (+3 ºC) and acidified (-0.3 pH unit) conditions. Gazeau et al. 2020, present the general setup of the experiments and the impacts of dust seeding and/or future climate change scenario on nutrients and biological stocks. The effects of dust deposition on biological stocks were highly

different between the three stations and could not be attributed to differences in their degree of oligotrophy but rather to the initial metabolic state of the community. Furthermore, ocean acidification and warming did not drastically modify the composition of the autotrophic assemblage with all groups benefiting from warmer and acidified conditions, suggesting an exacerbation of effects from atmospheric dust deposition in the future. Similar to the stocks, the effects on biological rates were highly different between the three stations (Gazeau et al., in prep., this issue). Heterotrophic prokaryote production rates and enzymatic activities were significantly enhanced at all three stations following simulated dust deposition, especially under future climate conditions. Overall bacterial mortality (through grazing and viral lysis) was enhanced after dust addition under future climate conditions (Dinasquet et al., in prep., this issue). Microbial (prokaryotes and eukaryotes) community composition shifted overtime in response to the perturbations, compared to the control communities that remained relatively stable. No visible effect of dust deposition on primary production rates could be observed at station TYR while clear enhancements were observed at the two other stations (Gazeau et al., in prep., this issue). Finally, as for bacteria, pH and temperature exacerbated these effects at those stations (ION and FAST). Dust addition induced a strong increase in N_2 fixation rates that was similar both under present and future climate conditions at TYR and ION (Ridame et al., in prep., this issue): compared to unmodified tanks, observed mean stimulations were higher at TYR station (x 6) than at ION (x 3.3). At FAST, where the impact was modest under present conditions (+41-49%), the future conditions significantly enhanced the increase of N_2 fixation after dust seeding (+97-120%). These experiments also permitted to study the fate of some lithogenic elements associated with dust, allowing a first direct assessment of the low percentage of dissolution for thorium (~ 1%) and protactinium (< 6 %) after Saharan dust deposition in seawater (Roy-Barman et al., 2020). Unforeseen effects of temperature and/or pH on the release of thorium and rare earth elements in seawater led to a lower Th release and a higher light REE release under increased greenhouse conditions. Contrasted responses were observed: aluminum kept dissolving over the course of the experiment whereas thorium and light rare earth elements initially released in seawater were scavenged back on the particles.

6. Conclusion

The PEACETIME oceanographic expedition conducted in spring 2017 cruised over a 20° longitudinal gradient across the western and central Mediterranean Sea during the season characterized by strong stratification, low productivity and high probability of wet dust deposition. Those conditions were required in order to fulfill the objectives of the project aiming

at quantifying the biogeochemical processes at play after atmospheric deposition and its impact on ecosystem functioning. Different atmospheric situations were encountered during the cruise. In particular, luckily, three contrasted situations in term of atmospheric deposition characterized the long duration stations, allowing the acquisition of a large dataset under different dynamical and biogeochemical in situ conditions to explore the chemical and ecosystem response to deposition. Thanks to an adaptive strategy based on a large panel of atmosphere and ocean real time observations and forecast models, the track of the cruise was optimized from day to day. In particular, it was possible to reach on time an area located more than 800 km away where an event was forecasted and actually observed and sampled. In situ observations could be completed in a very relevant way by three dust addition experiments considering present and future climate conditions. All the studies performed on board closely involved scientists from different disciplines making these outputs truly interdisciplinary.

The PEACETIME process study is an important contribution to the SOLAS international program. It also provides input function at the ocean surface for GEOTRACES key tracers when Saharan dust is deposited over the ocean and taking into account the biological activity and the impact of climate change. It will contribute to significantly improve the tracer-based mapping of lithogenic dust deposition over the ocean.

Acknowledgments

This study is a contribution to the PEACETIME project (http://peacetime-project.org), a joint initiative of the MERMEX and ChArMEx components supported by CNRS-INSU, IFREMER, CEA, and Météo-France as part of the programme MISTRALS coordinated by INSU. PEACETIME was endorsed as a process study by GEOTRACES. PEACETIME cruise https://doi.org/10.17600/17000300. We thank the captain and the crew of the RV Pourquoi Pas? for their professionalism and their work at sea. We warmly thank Louise Rousselet, Alain de Verneil, and Alice Della Penna for their precious help with SPASSO and the daily bulletins, Hélène Ferré from OMP/SEDOO for her management of the Peacetime Operation Center, and Louis Prieur for fruitful discussion on the characterisation of the ocean processes observed at the station FAST. We finally acknowledge the technical help of the many teams supporting operational production of model forecasts and remote sensing products that contributed to the POC and were the basis of our daily briefings and decision for the Fast Action, especially Jacques Descloitres for MSG-derived AOD, Louis Gonzalez for NASCube products, and Christos Spyrou for SKIRON forecasts.

Author contribution: CG and KD designed the PEACETIME project. FD and FDO analyzed the FAST Action. FD, MM and PN analysed the atmospheric components and VT, AD, AP and SB analysed the marine components. CG and KD prepared the manuscript with contributions from all co-authors.

Competing interests. The authors declare that they have no conflict of interest

Data availability. Underlying research data are being used by participants of the "PEACETIME" campaign to prepare other manuscripts, and therefore data are not publicly accessible at the time of publication. Data will be accessible (http://www.obs-vlfr.fr/proof/php/PEACETIME/peacetime.php, last access: 22 September 2020) once the special issue is completed (fall 2020). The policy of the database is detailed here http://www.obs-vlfr.fr/proof/dataconvention.php (last access: 22 September 2020).

References

1. Avila, A., Queralt-Mitjans, I., & Alarcón, M. (1997) Mineralogical composition of African dust delivered by red rains over northeastern Spain, J. Geophys. Res., 102, 21977-21996, doi:10.1029/97JD00485.
2. Barbieux M., Uitz J., Mignot A., Gentili B., Claustre H., Roesler C., Taillandier V., D'Ortenzio F., Loisel H., Poteau A., Leymarie E., Penkerc'h C., Schmechtig C. & Bricaud A., Biological production in two contrasted regions of the Mediterranean Sea during the oligotrophic period : An estimate based on the diel cycle of An estimate based on the diel cycle of optical properties measured by BGC-Argo profiling floats, in preparation (this special issue)
3. Bergametti G., E. Remoudaki, R. Losno, E. Steiner, B. Chatenet, & P. Buat-Ménard (1992) Source, transport and deposition of atmospheric phosphorus over the northwestern Mediterranean, Journal of Atmospheric Chemistry, 14, 501-513, doi:10.1007/BF00115254.
4. Bergametti, G., Dutot, A. L., Buat-Ménard, P., Losno, R., & Remoudaki, E. (1989) Seasonal variability of the elemental composition of atmospheric aerosol particles over the Northwestern Mediterranean, Tellus, 41B, 353-361, doi:10.1111/j.1600-0889.1989.tb00314.x.
5. Berline L, Doglioli AM, Petrenko A, Barrillon S, Simon-Bot F, Lemoigne, F, Espinasse B & Carlotti F,, Long distance particle transport to the Central Ionian Sea, , in preparation (this special issue)

6. Blanke, B., & Raynaud, S. (1997) Kinematics of the Pacific equatorial undercurrent: An Eulerian and Lagrangian approach from GCM results, Journal of Physical Oceanography, 27, 1038-1053, doi:10.1175/1520-0485(1997)027<1038:KOTPEU>2.0.CO;2.
7. Blanke, B., Arhan, M., Madec, G., & Roche, S. (1999) Warm water paths in the equatorial Atlantic as diagnosed with a general circulation model, Journal of Physical Oceanography, 29, 2753-2768, doi:10.1175/1520-0485(1999)029<2753:WWPITE>2.0.CO;2.
8. Bonnet, S., & Guieu, C. (2006) Atmospheric Forcing on the Annual Iron Cycle in the Mediterranean Sea. A one-year Survey. Journal of Geophysical Research, 111, C09010, doi:10.1029/2005JC003213.
9. Bosc, E., Bricaud, A., & Antoine, D. (2004) Seasonal and interannual variability in algal biomass and primary production in the Mediterranean Sea, as derived from 4 years of SeaWiFS observations, Global Biogeochemical Cycles, 18, GB1005, doi:10.1029/2003GB002034.
10. Brandt M.I, Trouche B., Quintric L., Wincker P., Poulain J., Arnaud-Haond S., A flexible pipeline combining bioinformatic correction tools for prokaryotic and eukaryotic metabarcoding. https://doi.org/10.1101/717355, 2019
11. Bressac M, Wagener T, Tovar-Sanchez A, Ridame C, Jacquet S, Dufour A, Albani S, Fu F, Desboeufs K & Guieu C., , Residence time of iron and aluminium in the surface Mediterranean Sea (Peacetime cruise), in preparation (this special issue)
12. Bressac M., C. Guieu, D. Doxaran, F. Bourrin, N. Leblond K. Desboeufs & C. Ridame (2014) Quantification of the lithogenic carbon pump following a simulated dust deposition event in large mesocosm, Biogeosciences, 11, 1007-1020, doi:10.5194/bg-11-1007-2014.
13. Bressac M., C. Guieu, M. J. Ellwood, A. Tagliabue, T. Wagener, E. C. Laurenceau Cornec, H. Whitby, G. Sarthou, & P. W. Boyd. (2019) Resupply of mesopelagic dissolved iron controlled by particulate iron composition. Nature Geoscience, 12(12), 995:1000, doi:10.1038/s41561-019-0476-6.
14. Bressac, M., & Guieu, C. (2013) Post-depositional processes: What really happens to new atmospheric iron in the ocean surface? Global Biogeochemical Cycles, 27, 859-870, doi:10.1002/gbc.20076.
15. de Verneil, A., Rousselet, L., Doglioli, A. M., Petrenko, A. A., Maes, C., Bouruet-Aubertot, P., & Moutin, T. (2018) OUTPACE long duration stations: physical

variability, context of biogeochemical sampling, and evaluation of sampling strategy, Biogeosciences, 15, 2125–2147, doi:10.5194/bg-15-2125-2018.

16. Desboeufs K., J.-F. Doussin, S. Triquet, C. Giorio, Y. Fu, F.Dulac, D. Garcia-Nieto, P. Chazette, A. Féron, P. Formenti, C. Gaimoz, F. Maisonneuve, V. Riffault, A. Saiz-Lopez, G. Siour, P. Zapf and C. Guieu, ProcEss studies at the Air-sEa Interface after dust deposition in the MEditerranean sea (PEAcEtIME) cruise: Atmospheric and FAST ACTION overview and illustrative observations, in preparation (this special issue)
17. Desboeufs K., N. Leblond, T. Wagener, E. Bon Nguyen & C. Guieu (2014) Chemical fate and settling of mineral dust in surface seawater after atmospheric deposition observed from dust seeding experiments in large mesocosms, Biogeosciences, 11, 5581-5594, doi:10.5194/bg-11-5581-2014.
18. Desboeufs, K., Bon Nguyen, E., Chevaillier, S., Triquet, S., & Dulac, F. (2018) Fluxes and sources of nutrient and trace metal atmospheric deposition in the northwestern Mediterranean, Atmospheric Chemistry and Physics, 18, 14477–14492, doi:10.5194/acp-18-14477-2018.
19. Dinasquet J., Bigeard E., Gazeau, F., Marañón E., Ridame C., Van Wambeke F., Obernosterer I. & Baudoux A-C., Impact of dust enrichment on the microbial food web under present and future conditions of pH and temperature, in preparation (this special issue)
20. Doglioli, A. M., Nencioli, F., Petrenko, A. A., Rougier, G., Fuda, J. L., & Grima, N. (2013) A software package and hardware tools for in situ experiments in a Lagrangian reference frame. Journal of Atmospheric and Oceanic Technology, 30, 1940-1950, doi:10.1175/JTECH-D-12-00183.1.
21. d'Ortenzio, F., Iudicone, D., de Boyer Montegut, C., Testor, P., Antoine, D., Marullo, S., Santoleri, R., & Madec, G. (2005) Seasonal variability of the mixed layer depth in the Mediterranean Sea as derived from in situ profiles, Geophysical Research Letters, 32, L12605, doi:10.1029/2005GL022463.
22. d'Ovidio, F., Della Penna, A., Trull, T. W., Nencioli, F., Pujol, M.-I., Rio, M.-H., Park, Y.-H., Cotté, C., Zhou, M., & Blain, S. (2015) The biogeochemical structuring role of horizontal stirring: Lagrangian perspectives on iron delivery downstream of the Kerguelen Plateau, Biogeosciences, 12, 5567–5581, 2015, doi:10.5194/bg-12-5567-2015.
23. Dulac F., C. Moulin, H. Planquette, M. Schulz, & M. Tartar (2004) African dust deposition and ocean colour in the eastern Mediterranean. Rapp. Comm. Int. Mer

Médit., Vol. 37, 190, Commission Internationale pour l'Exploration Scientifique de la Méditerranée, Monaco.

24. Feliú, G., Pagano, M., Hidalgo, P., and Carlotti, F. (2020) Structure and functioning of epipelagic mesozooplankton and response to dust events during the spring PEACETIME cruise in the Mediterranean Sea, Biogeosciences, https://doi.org/10.5194/bg-2020-126, accepted, 2020.
25. Formenti, P., D'Anna, B., Flamant, C., Mallet, M., Piketh, S. J., Schepanski, K., ... & Chaboureau, J. P. (2019) The Aerosols, Radiation and Clouds in southern Africa (AEROCLO-sA) field campaign in Namibia: overview, illustrative observations and way forward, Bulletin of the American Meteorological Society, 100, 1277-1298, doi:10.1175/BAMS-D-17-0278.1.
26. Freney E., Sellegri K., Nicossia A., Trueblood J., Rinaldi M., Williams L., Prevot A., Thyssen M., Gregori G., Haentjens N., Dinasquet J., Obernosterer I., Van-Wambeke F., Engel A., Zancker B., Desboeufs K., Asmi E., Timmonen H., and Guieu C., 2020, Mediterranean nascent sea spray organic aerosol and relationships with seawater biogeochemistry, Atmos. Chem. Phys. Discuss., https://doi.org/10.5194/acp-2020-406, in review, 2020.
27. Fu, Y., Desboeufs, K., Vincent, J., Bon Nguyen, E., Laurent, B., Losno, R., & Dulac, F. (2017) Estimating chemical composition of atmospheric deposition fluxes from mineral insoluble particles deposition collected in the western Mediterranean region, Atmospheric Measurement Techniques, 10, 4389–4401, doi:10.5194/amt-10-4389-2017.
28. Fu F., S. Triquet, J.-F. Doussin, C. Giorio, F. Dulac, M. Bressac, A. Tovar-Sanchez and Karine Desboeufs, Wet deposition of nutrients and trace metals in the Mediterranean Sea during PEACETIME cruise: anthropogenic vs dusty rains, in preparation (a) (this special issue)
29. Fu F., Triquet S., Doussin J-F, Giorio C., Guieu C. & Desboeufs K., Aerosols characterisation and dry deposition of trace metals and nutrients in remote Mediterranean Sea, in preparation (b) (this special issue).
30. Gallisai, R., Peters, F., Volpe, G., Basart, S., & Baldasano, J. M. (2014) Saharan dust deposition may affect phytoplankton growth in the Mediterranean Sea at ecological time scales. PloS ONE, 9, e110762, doi:10.1371/journal.pone.0110762, 2014.

31. Garel, M., Bonin, P., Martini, S., Guasco, S., Roumagnac, M., Bhairy, N., ... & Tamburini, C. (2019). Pressure-Retaining Sampler and High-Pressure Systems to Study Deep-Sea Microbes Under in situ Conditions. Frontiers in microbiology, 10, 453.
32. Gazeau F, Ridame C., Van Wambeke F., Alliouane S., Stolpe C., Irisson JO, Marro S., Grisoni JM, De Liège G., Nunige S., Djaoudi K., Pulido-Villena E., Dinasquet J., Obernosterer I., Catala P., and Guieu C.. (2020) Impact of dust enrichment on Mediterranean plankton communities under present and future conditions of pH and temperature : an experimental overview, Biogeosciences Discuss., https://doi.org/10.5194/bg-2020-202, in review, 2020.
33. Gazeau F., Marañon E., Van Wambeke F., Alliouane S., Stolpe C., Blasco T., Ridame C., Pérez-Lorenzo M., Barbara Marie, Engel A., Zäncker B., & Guieu C. Impact of dust enrichment on carbon budget and metabolism of Mediterranean plankton communities under present and future conditions of pH and temperature, in preparation (this special issue)
34. Guerzoni, S., Chester, R., Dulac, F., Herut, B., Loÿe-Pilot, M. D., Measures, C., Migon, C., Molinaroli, E., Moulin, C., Rossini, P., Saydam, C., Soudine, A., & Ziveri, P. (1999) The role of atmospheric deposition in the biogeochemistry of the Mediterranean Sea, Progress in Oceanography, 44, 147-190, doi:10.1016/S0079-6611(99)00024-5.
35. Guerzoni, S., Quarantotto, G., Molinaroli, E., & Rampazzo, G. (1995) More data on source signature and seasonal fluxes to the Central Mediterranean Sea of aerosol dust originated in desert areas, in Water Poll. Res. Rep., 32, J.-M. Martin and H. Barth Eds., 253-260.
36. Guieu, C., Bonnet, S., Wagener, T., & Loÿe-Pilot, M.D. (2005) Biomass burning as a source of dissolved iron to open ocean? Geophysical Research Letters, 32, L19608, doi:10.1029/2005GL022962.
37. Guieu, C., Loÿe-Pilot, M-D, Benyaya, L., & Dufour, A. (2010) Spatial and temporal variability of atmospheric fluxes of metals (Al, Fe, Cd, Zn and Pb) and phosphorus over the whole Mediterranean from a one-year monitoring experiment; Biogeochemical implications, Marine Chemistry, 120, 164-178, doi:10.1016/j.marchem.2009.02.004.
38. Guieu, C., Aumont, O., Paytan, A., Bopp, L., Law, C.S., Mahowald, N., Achterberg, E.P., Marañón, E., Salihoglu, B., Crise, A., Wagener, T., Herut, B., Desboeufs, K., Kanakidou, M., Olgun, N., Peters, F., Pulido-Villena, E., Tovar-Sanchez, A,. & Völker, C. (2014a) The significance of episodicity in atmospheric deposition to Low Nutrient

Low Chlorophyll regions, Global Biogeochemical Cycles, 2014, doi:10.1002/2014GB004852.

39. Guieu C., Ridame, C., Pulido-Villena, E., Bressac, M., Desboeufs, K., & Dulac, F. (2014b) Impact of dust deposition on carbon budget: a tentative assessment from a mesocosm approach, Biogeosciences, 11, 5621-5635, doi:10.5194/bg-11-5621-2014.
40. Guieu, C. and Ridame, C., (2020), Impact of atmospheric deposition on marine chemistry and biogeochemistry, in: Atmospheric Chemistry in the Mediterranean Region: Comprehensive Diagnosis and Impacts, edited by F. Dulac, S. Sauvage, and E. Hamonou, Springer, Cham, Switzerland, in press
41. Holben, B.N., Eck, T.F., Slutsker, I., Tanré, D., Buis, J.P., Setzer, A., Vermote, E., Reagan, J.A., Kaufman, Y.J., Nakajima, T., Lavenu, F., Jankowiak, I., & Smirnov, A. (1998) AERONET—A federated instrument network and data archive for aerosol characterization, Remote Sensing of Environment, 66, 1-16, doi:10.1016/S0034-4257(98)00031-5.
42. Jacquet S, Garel M, Tamburini C, A. Dufour, N. Bhairy, S. Gasco & D. Lefèvre, Particulate biogenic barium and carbon remineralization fluxes at mesopelagic depths during the PEACETIME cruise, submitted to Biogeoscience this special issue (MS No. bg-2020-271
43. Jordi, A., Basterretxea, G., Tovar-Sánchez, A., Alastuey, A., & Querol, X. (2012) Copper aerosols inhibit phytoplankton growth in the Mediterranean Sea, Proc. of the National Academy of Sciences, 109, 21246-21249, doi: 10.1073/pnas.1207567110.
44. Kouvarakis, G., Mihalopoulos, N., Tselepides, T., & Stavrakakis, S. (2001) On the importance of atmospheric nitrogen inputs on the productivity of eastern Mediterranean, Global Biogeochemical Cycles, 15, 805–818, doi:10.1029/2001GB001399.
45. Kubilay N., S. Nickovic, C. Moulin, & F. Dulac (2000) An illustration of the transport and deposition of mineral aerosol onto the eastern Mediterranean, Atmospheric Environment, 34, 1293-1303, doi:10.1016/S1352-2310(99)00179-X.
46. Law, C.S., Brévière E., de Leeuw, G., Garçon V., Guieu, C., Kieber, D.J., Kontradowitz, S., Paulmier, A., Quinn, P.K., Saltzman, E.S., Stefels, J., & von Glasow, R. (2013) Evolving Research Directions in Surface Ocean-Lower Atmosphere (SOLAS) Science, Environmental Chemistry, 10, 1-16, doi:10.1071/EN12159.
47. Long, M. S., Keene, W. C., Kieber, D. J., Frossard, A. A., Russell, L. M., Maben, J. R., Kinsey, J. D., Quinn, P. K., and Bates, T. S. (2014), Light-enhanced primary marine

aerosol production from biologically productive seawater, *Geophys. Res. Lett.*, 41, 2661– 2670, doi:10.1002/2014GL059436.

48. Louis J., Bressac, M., Pedrotti, M.L., & Guieu, C. (2015) Dissolved inorganic nitrogen and phosphorus dynamics in abiotic seawater following an artificial Saharan dust deposition, Frontiers in Marine Sciences, 2, 27, doi:10.3389/fmars.2015.00027.
49. Louis, J., Pedrotti, M. L., Gazeau, F., & Guieu, C. (2017) Experimental evidence of formation of Transparent Exopolymer Particles (TEP) and POC export provoked by dust addition under current and high pCO2 conditions, PloS one, 12, e0171980, doi:10.1371/journal.pone.0171980.
50. Loÿe-Pilot, M. D., Martin, J. M., & Morelli, J. (1986) Influence of Saharan dust on the rain acidity and atmospheric input to the Mediterranean, Nature, 321, 427-428, doi:10.1038/321427a0.
51. Loÿe-Pilot, M.-D., & Martin, J.-M. (1996) Saharan dust input to the western Mediterranean: an eleven years record in Corsica, in The Impact of Desert Dust Across the Mediterranean, S. Guerzoni and R. Chester Eds., Kluwer, 191-199.
52. Mallet, M., et al. (2016) Overview of the Chemistry-Aerosol Mediterranean Experiment/Aerosol Direct Radiative Forcing on the Mediterranean Climate (ChArMEx/ADRIMED) summer 2013 campaign, Atmospheric Chemistry and Physics, 16, 455–504, doi:10.5194/acp-16-455-2016.
53. Marañón E, Pérez-Lorenzo M, Van Wambeke F, Uitz J, Dinasquet J, Haëntjens N, Dimier C, Deep maxima of phytoplankton biomass, primary production and bacterial production in the Mediterranean sea during late spring, Biogeosciences Discuss., https://doi.org/10.5194/bg-2020-261, in review, 2020.
54. Markaki, Z., Oikonomou, K., Kocak, M., Kouvarakis, G., Chaniotaki, A., Kubilay, N., & Mihalopoulos, N. (2003) Atmospheric deposition of inorganic phosphorus in the Levantine Basin, eastern Mediterranean: Spatial, temporal variability, and its role in seawater productivity, Limnology and Oceanography, 48, 1557–1568, doi:10.4319/lo.2003.48.4.1557.
55. Markaki, Z., Loÿe-Pilot, M. D., Violaki, K., Benyahya, L., & Mihalopoulos, N. (2010) Variability of atmospheric deposition of dissolved nitrogen and phosphorus in the Mediterranean and possible link to the anomalous seawater N/P ratio, Marine Chemistry, 120, 187-194, doi:10.1016/j.marchem.2008.10.005.

56. Menna, M., Poulain, P. M., Ciani, D., Doglioli, A., Notarstefano, G., Gerin, R., ... & Drago, A. (2019). New insights of the Sicily Channel and southern Tyrrhenian Sea variability. Water, 11(7), 1355.
57. Moon, J. Y., Lee, K., Tanhua, T., Kress, N., and Kim, I. N. (2016)Temporal nutrient dynamics in the Mediterranean Sea in response to anthropogenic inputs, Geophysical Research Letters, 43, 5243–5251, doi:10.1002/2016GL068788.
58. Morales-Baquero, R., & Pérez-Martínez, C. (2016) Saharan versus local influence on atmospheric aerosol deposition in the southern Iberian Peninsula: Significance for N and P inputs, Global Biogeochemical Cycles, 30, 501-513, doi: 10.1002/2015GB005254.
59. Moulin, C., Lambert, C. E., Dayan, U., Masson, V., Ramonet, M., Bousquet, P., Legrand, M., Balkanski, Y.J., Guelle, W., Marticorena, B., Bergametti, G., & Dulac, F. (1998) Satellite climatology of African dust transport in the Mediterranean atmosphere. Journal of Geophysical Research: Atmospheres, 103, 13137-13144, doi:10.1029/98JD00171.
60. Moutin, T., Doglioli, A. M., De Verneil, A., & Bonnet, S. (2017) Preface: The Oligotrophy to the UlTra-oligotrophy PACific Experiment (OUTPACE cruise, 18 February to 3 April 2015), doi:10.5194/bg-14-3207-2017.
61. Nabat, P., Somot, S., Mallet, M., Michou, M., Sevault, F., Driouech F., Meloni, D., Di Sarra, A., Di Biagio, C., Formenti, P., Sicard, M., Léon, J.-F. and Bouin, M.-N. (2015), Dust aerosol radiative effects during summer 2012 simulated with a coupled regional aerosol-atmosphere-ocean model over the Mediterranean region, Atm. Chem. Phys., 15, 3303-3326, doi:10.5194/acp-15-3303-2015.
62. Nencioli, F., d'Ovidio, F., Doglioli, A. M., & Petrenko, A. A. (2011) Surface coastal circulation patterns by in-situ detection of Lagrangian coherent structures, Geophysical Research Letters, 38, L17604, doi:10.1029/2011GL048815.
63. Petrenko, A.A., Doglioli AM, Nencioli F., Kersalé M., Hu Z., & d'Ovidio F. (2017) A review of the LATEX project: mesoscale to submesoscale processes in a coastal environment, Ocean Dynamics, 67, 513-533, doi:10.1007/s10236-017-1040-9.
64. Pey, J., Querol, X., Alastuey, A., Forastiere, F., & Stafoggia, M. (2013) African dust outbreaks over the Mediterranean Basin during 2001–2011: PM10 concentrations, phenomenology and trends, and its relation with synoptic and mesoscale meteorology. Atmospheric Chemistry and Physics, 13, 1395-1410, doi:10.5194/acp-13-1395-2013.

65. Pitta, P., Kanakidou, M., Mihalopoulos, N., Christodoulaki, S., Dimitriou, P. D., Frangoulis, C., Giannakourou, A., Kagiorgi, M., Lagaria, A., Nikolaou, P., Papageorgiou, N., Psarra, S., Santi, I, Tsapakis, M., Tsiola, A., Viollaki, K., & Petihakis, G. (2017) Saharan dust deposition effects on the microbial food web in the Eastern Mediterranean: a study based on a mesocosm experiment. Frontiers in Marine Science, 4, 117, doi:10.3389/fmars.2017.00117.
66. Pulido-Villena E., A.-C. Baudoux, I. Obernosterer, M. Landa, J. Caparros, P. Catala, C. Georges, J. Harmand, & C. Guieu (2014) Microbial food web dynamics in response to a Saharan dust event: results from a mesocosm study in the oligotrophic Mediterranean Sea, Biogeosciences, 11, 5607–5619, doi:10.5194/bg-11-5607-2014.
67. Pulido-Villena, E., Van Wambeke, F., Desboeufs, K., Djaoudi, K., Taillandier, V., Barrillon, S., Doglioli, A., D'Ortenzio, F., Estournel, C., Fu, Y., Gaillard, T., Guasco, S., Marsaleix, P., Nunige, S., Petrenko, A.,Raimbault, P., Triquet, S., Guieu, C, Analysis of external and internal sources contributing to phosphate supply to the upper waters of the Mediterranean Sea (Peacetime cruise), in preparation (this special issue)
68. Richon, C., J.-C. Dutay, F. Dulac, R. Wang, Y. Balkanski, P. Nabat, O. Aumont, K. Desboeufs, B. Laurent, C. Guieu, P. Raimbault, & J. Beuvier (2018a) Modeling the impacts of atmospheric deposition of nitrogen and desert dust-derived phosphorus on nutrients and biological budgets of the Mediterranean Sea, Progress in Oceanography, 163, 21-39, doi:10.1016/j.pocean.2017.04.009.
69. Richon, C., Dutay, J.-C., Dulac, F., Wang, R., & Balkanski, Y (2018b) Modeling the biogeochemical impact of atmospheric phosphate deposition from desert dust and combustion sources to the Mediterranean Sea, Biogeosciences, 15, 2499–2524, https://doi.org/10.5194/bg-15-2499-2018.
70. Ridame, C., M. Le Moal, C. Guieu, E. Ternon, I. C. Biegala, S. L'Helguen, & M. Pujo-Pay (2011) Nutrient control of N2 fixation in the oligotrophic Mediterranean Sea and the impact of Saharan dust events, Biogeosciences, 8, 2773-2783, doi:10.5194/bg-8-2773-2011.
71. Ridame, C., Guieu, C. & S. L'Helguen (2013) Strong stimulation of N2 fixation in oligotrophic Mediterranean Sea: results from dust addition in large in situ mesocosms, Biogeosciences, 10, 7333–7346, doi: 10.5194/bg-10-7333-2013.
72. Ridame, C., Dekaezemacker, J., Guieu, C., Bonnet, S., l'Helguen, S., & Malien, F. (2014). Contrasted Saharan dust events in LNLC environments: impact on nutrient

dynamics and primary production. Biogeosciences, *11*(17), 4783-4800. doi:10.5194/bg-11-4783-2014101.

73. Ridame C., Dinasquet J., Bigeard E., Hallstrom, S., Riemann L.,Tovar-Sanchez A., Gazeau F. Baudoux A-C., Guieu C., Impact of dust enrichment on N2 fixation and diversity of diazotrophs under present and future conditions of pH and temperature, in preparation, (this special issue)
74. Rousselet, L., Doglioli, A. M., de deVerneil, A., Pietri, A., Della Penna, A., Berline, L., Marrec, P., Grégori, G., Thyssen, M., Carlotti, F., Barrillon, S., Simon-Bot, F., Bonal, M., D'Ovidio, F., & Petrenko, A. (2019) Vertical motions and their effects on a biogeochemical tracer in a cyclonic structure finely observed in the Ligurian Sea, Journal of Geophysical Research: Oceans, 124, 3561-3574, doi: 10.1029/2018JC014392.
75. Roy-Barman M., Foliot L., Douville E., Leblond N., Gazeau F., Bressac M., Wagener T., Ridame C., Desboeufs K. & Guieu C., Contrasted release of insoluble elements (Fe, Al, REE, Th, Pa) after dust deposition in seawater: a tank experiment approach, Biogeosciences Discuss., https://doi.org/10.5194/bg-2020-247, in review, 2020.Sellegri K., Nicosia A., Freney E., Uitz J., Thyssen M., Grégori G., , Engel A., Zäncker B., Haëntjens N., Mas S., Picard D., Saint-Macary A., Peltola M., Rose C., Trueblood J., Lefevre D., D'Anna B., Desboeufs K., Meskhidze N., Guieu C. and Law C., Linking living microorganisms of the Ocean and atmospheric Cloud Condensation Nuclei production, Sc. Rep. in revision, 2020
76. SOLAS 2015-2025: Science Plan and Organisation (2015) SOLAS Scientific Steering Committee and Emilie Brévière (Editors) SOLAS International Project Office, Kiel. 68 pp.
77. Taillandier V., Prieur L. D'Ortenzio F., Ribera d'Alcalà M., and Pulido-Villena E., Profiling float observation of thermohaline staircases in the western Mediterranean Sea and impact on nutrient fluxes, Biogeosciences, 17, 3343–3366, https://doi.org/10.5194/bg-17-3343-2020, 2020
78. Taupier-Letage, I., I. Puillat, C. Millot, and P. Raimbault, Biological response to mesoscale eddies in the Algerian Basin, J. Geophys. Res., 108(C8), 3245, doi:10.1029/1999JC000117, 2003.
79. Ternon E. , Guieu, C., Loÿe-Pilot, M-D., Leblond, N., Bosc, E., Gasser, B., Martin, J., & Miquel, J.-C. (2010) The impact of Saharan dust on the particulate export in the water

column of the North Western Mediterranean Sea, Biogeosciences, 7, 809-826, doi: 10.5194/bg-7-809-2010.

80. Testor P., Send, U., Gascard, J.-C., Millot, C., Taupier-Letage, I., & Béranger, K. (2005) The mean circulation of the southwestern Mediterranean Sea: Algerian Gyres, Journal of Geophysical Research, 110, C110017, doi:10.1029/2004JC002861.
81. The MERMEX Group (2011) Marine ecosystems' responses to climatic and anthropogenic forcings in the Mediterranean, Progress in Oceanography, 91, 97-166, doi:10.1016/j.pocean.2011.02.003.
82. Tovar-Sánchez, A., Arrieta, J.M., Duarte, C.M., & Sañudo-Wilhelmy, S.A. (2014) Spatial gradients in trace metal concentrations in the surface microlayer of the Mediterranean Sea, Frontiers in Marine Science, 1, 79, doi: 10.3389/fmars.2014.00079.
83. Tovar-Sánchez A., A Rodríguez-Romero, A Engel, B Zäncker, F Fu, E Marañón, M Pérez-Lorenzo, M Bressac, T Wagener, K Desboeuf, S Triquet, G Siour, K. Desboeufs, C Guieu, (2020) Characterising the surface microlayer in the Mediterranean Sea: trace metals concentration and microbial plankton abundance, Biogeosciences, 17, 2349–2364, doi.org/10.5194/bg-17-2349-2020
84. Trueblood J., Nicosia, A., Engel A., Zäncker B., Rinaldi M., Thyssen M., Obernosterer I., Dinasquet J., E. Freney, Belosi F. Tovar-Sanchez A., Rodriguez-Romero A., Santachiara G., C. Guieu & K. sellegri; (2020) A Two-Component Parameterization of Marine Ice Nucleating Particles Based on Seawater Biology and Sea Spray Aerosol Measurements in the Mediterranean Sea, Atmos. Chem. Phys. Discuss., https://doi.org/10.5194/acp-2020-487, 2020, in revision, 2020
85. Tsagaraki, T. M., Herut, B., Rahav, E., Berman Frank, I. R., Tsiola, A., Tsapakis, M.; Giannakourou, A., Gogou, A., Panagiotopoulos, C., Violaki, K.; et al. (2017) Atmospheric Deposition Effects on Plankton Communities in the Eastern Mediterranean: A Mesocosm Experimental Approach, Frontiers in Marine Science 2017, 4, 210. https://doi.org/10.3389/fmars.2017.00210.
86. Tsapakis, M., Apsotolaki, M., Eisenreich, S., & Stephanou, E.G. (2006) Atmospheric deposition and marine sedimentation fluxes of polycyclic aromatic hydrocarbons in the Eastern Mediterranean Basin. Environmental Science and Technology 40, 4922-4927.
87. Van Wambeke F., Pulido E., Desboeufs K., Dinasquet J. Djaoudi K., Engel A., Garel M., Guasco S., Helias-Nunige S., Taillandier V., Zäncker B., Tamburini C. (2020) Spatial patterns of biphasic ectoenzymatic kinetics in link with biogeochemical properties within surface, deep chlorophyll maximum layer, Levantine intermediate

waters and deep waters in the Mediterranean Sea in spring, Biogeosciences Discuss., https://doi.org/10.5194/bg-2020-253, in review, 2020.

88. Van Wambeke F., Taillandier V., Desboeufs K., Pulido-Villena E., Dinasquet J, Engel A., Maranon,., Ridame C., and Guieu C., Influence of atmospheric deposition on biogeochemical cycles in an oligotrophic ocean system, in preparation, this issue
89. Varga, G., Újvári, G., & Kovács, J. (2014) Spatiotemporal patterns of Saharan dust outbreaks in the Mediterranean Basin, Aeolian Research, 15, 151-160, doi:10.1016/j.aeolia.2014.06.005.
90. Vincent, J., Laurent, B., Losno, R., Bon Nguyen, E., Roullet, P., Sauvage, S., Chevaillier, S., Coddeville, P., Ouboulmane, N., di Sarra, A. G., Tovar-Sánchez, A., Sferlazzo, D., Massanet, A., Triquet, S., Morales Baquero, R., Fornier, M., Coursier, C., Desboeufs, K., Dulac, F., & Bergametti, G. (2016) Variability of mineral dust deposition in the western Mediterranean basin and south-east of France, Atmospheric Chemistry and Physics, 16, 8749-8766, doi:10.5194/acp-16-8749-2016.
91. Violaki K., Zarbas, P., & Mihalopoulos, N. (2010) Long-term measurements of water-soluble organic nitrogen (WSON) in atmospheric deposition in the Eastern Mediterranean: Fluxes, origin and biogeochemical implications, Marine Chemistry, 120, 179–186, doi:10.1016/j.marchem.2009.08.004.
92. Wagener, T., Guieu C., & Leblond N. (2010) Effects of dust deposition on iron cycle in the surface Mediterranean Sea: results from a mesocosm seeding experiment, Biogeosciences, 7, 3769-3781, doi: 10.5194/bg-7-3769-2010.
93. Wuttig K., Wagener, T., Bressac, M., Dammshäuser, A., Streu, P., Guieu, C., & Croot, P.L. (2013) Impacts of dust deposition on dissolved trace metal concentrations (Mn, Al and Fe) during a mesocosm experiment, Biogeosciences 10, 2583-2600, doi:10.5194/bg-10-2583-2013.
94. Zäncker B., Cunliffe M., Engel A., Eukaryotic Community Composition in the sea surface microlayer across an east-west gradient in the Mediterranean Sea, Biogeosciences Discuss., https://doi.org/10.5194/bg-2020-249, in review, 2020.

Table 1. Date of occupation, position and depth of the short stations (ST1-ST10), of the long stations (TYR, ION, FAST) and of the SAV station.

	arrival date	local time	departure date	local time	depth m	lat N	long E
ST1	12/05/2017	05:45	12/05/2017	21:15	1580	41°53.5	6°20

ST2	13/05/2017	06:30	13/05/2017	13:08	2830	40°30.36	6°43.78
ST3	14/05/2017	06:00	14/05/2017	13:30	1404	39°08.0	7°41.0
ST4	15/05/2017	05:56	15/05/2017	13:04	2770	37°59.0	7°58.6
ST5	16/05/2017	04:00	16/05/2017	10:58	2366	38°57.2	11°1.4
TYRR	17/05/2017	05:08	21/05/2017	15:59	3395	39°20.4	12°35.56
ST6	22/05/2017	04:50	22/05/2017	10:38	2275	38°48.47	14°29.97
SAV	23/05/2017	11:30	23/05/2017	14:17	2945	37°50.4	17°36.4
ST7	23/05/2017	21:10	24/05/2017	07:15	3627	36°39.5	18°09.3
ION	24/05/2017	18:02	29/05/2017	08:25	3054	35°29.1	19°47.77
ST8	30/05/2017	03:53	30/05/2017	09:41	3314	36°12.6	16°37.5
ST9	01/06/2017	19:13	02/06/2017	04:41	2837	38°08.1	5°50.5
FAST	02/06/2017	20:24	07/06/2017	23:25	2775	37°56.8	2°54.6
ST10	08/06/2017	05:12	08/06/2017	10:25	2770	37°27.58	1°34.0
FAST -bis	08/06/2017	21:06	09/06/2017	00:16	2775	37°56.8	2°55.0

Table 2. Overview of the work performed at sea during the PEACETIME cruise and associated publications.

Operations at sea	total number	**SHORT STATIONS**										**LONG STATIONS**				**Papers presenting the data**
		1	2	3	4	5	6	7	8	9	10	SAV	TYR	ION	FAST	
Atmospheric sampling	continuous	CONTINUOUS														*Desboeufs et al., in prep; Fu et al., in prep. (b);*
Rain water collection	2													X	X	*Fu et al., in prep (a)*
Continuous surface seawater pumping (-5 m)	continuous	CONTINUOUS														*Freney et al., 2020. Trueblood et al., 2020. Sellegri et al., in rev.*
Moving Vessel Profiler	a total of 1000 profiles while moving (0-300m)	between the short stations and in the long stations area as frequent as possible														*Guieu et al., this paper; Berline et al. in prep.*
Microlayer sampling (rubber boat)	17 sampling	X		X	X	X	X	X	X	X		X	XX	XX	XXXX	*Tovar-Sanchez et al., 2020; Zancker et al., 2020.*
Classical Rosette with 24 Niskin bottles or 22 Niskin bottles + 3 HP bottles (see details in section 5.1 work at sea).	90 casts	0-500 and 0-bottom														*Taillandier et al., 2020; van Wambeke et al., 2020.; Maranon et al., 2020.; Berline et al., in prep.; Jacquet et al., submitted.; Zancker et al., 2020.; Barbieux et al., in prep.; Guieu et al., this paper ; Garel et al., 2019(*)*
Trace metal Clean Rosette on kevlar cable with 24 teflon-coated GoFlo bottles [2].	27 casts	0-bottom														*Bressac et al., 2019. Whitby et al., 2020. Bressac et al., in prep.; Pulido-Villena et al., in prep.; Ridame et al., in prep.*
Zooplankton Net (0-200 m)	23 net tows	X	X	X	X	X	X	X	X	X			XXXX	XXXX	XXXX	*Feliu et al., 2020*
Optical measurements: HyperPro [3]	17 free-fall profiles	X	X	X	X	X	X					X	XXXX	XX	XXXX	
Drifting mooring	3 times												X	X	X	*Bressac et al., (2019). Whitby et al., 2020. Bressac et al., in prep.*
Marine snow catcher (depth m)	13												70 -80 - 90 -200	80 -100 - 150 - 200	70 -75 -80- 100	
Sediment Cores	3 times												X	X	X	*Brandt et al., 2019 (*)*
SVP (Surface Velocity Program) drifters	20 drifters												X	X		*Menna et al., 2019 (*). Guieu et al., this paper; Berline et al.in prep.*
Biogeochemical ARGO float	2 deployments, 1 recovery											X		X		*Taillandier et al., 2020. Barbieux et al., in prep.*
Surface seawater pumping (large volume (1800 L) for experiments in Climate Reactors)	3 times (long duration stations)												X	X	X	*Gazeau et al., 2020. Gazeau et al., in prep.; Ridame et al., in prep.; Roy-Barman et al., 2020.; Dinasquet et al., in prep.*

** Papers using PEACETIME data but not in close links with PEACETIME objectives, they will not be detailled in the section 6.*

Figures.

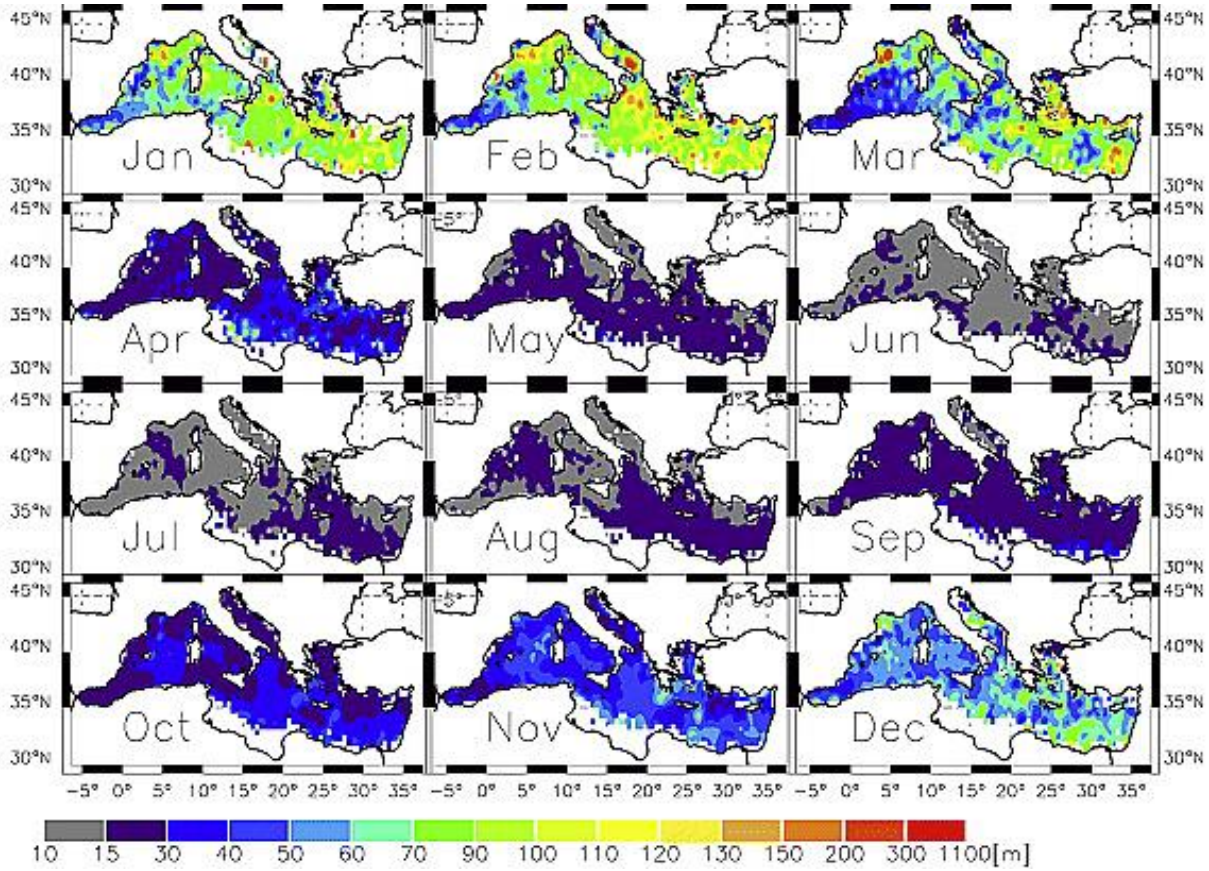

Figure 1. Mediterranean surface mixed layer depth (m) monthly climatology over 1940-2004 (in m; from D'Ortenzio et al., 2005; Copyright 2005 by the American Geophysical Union).

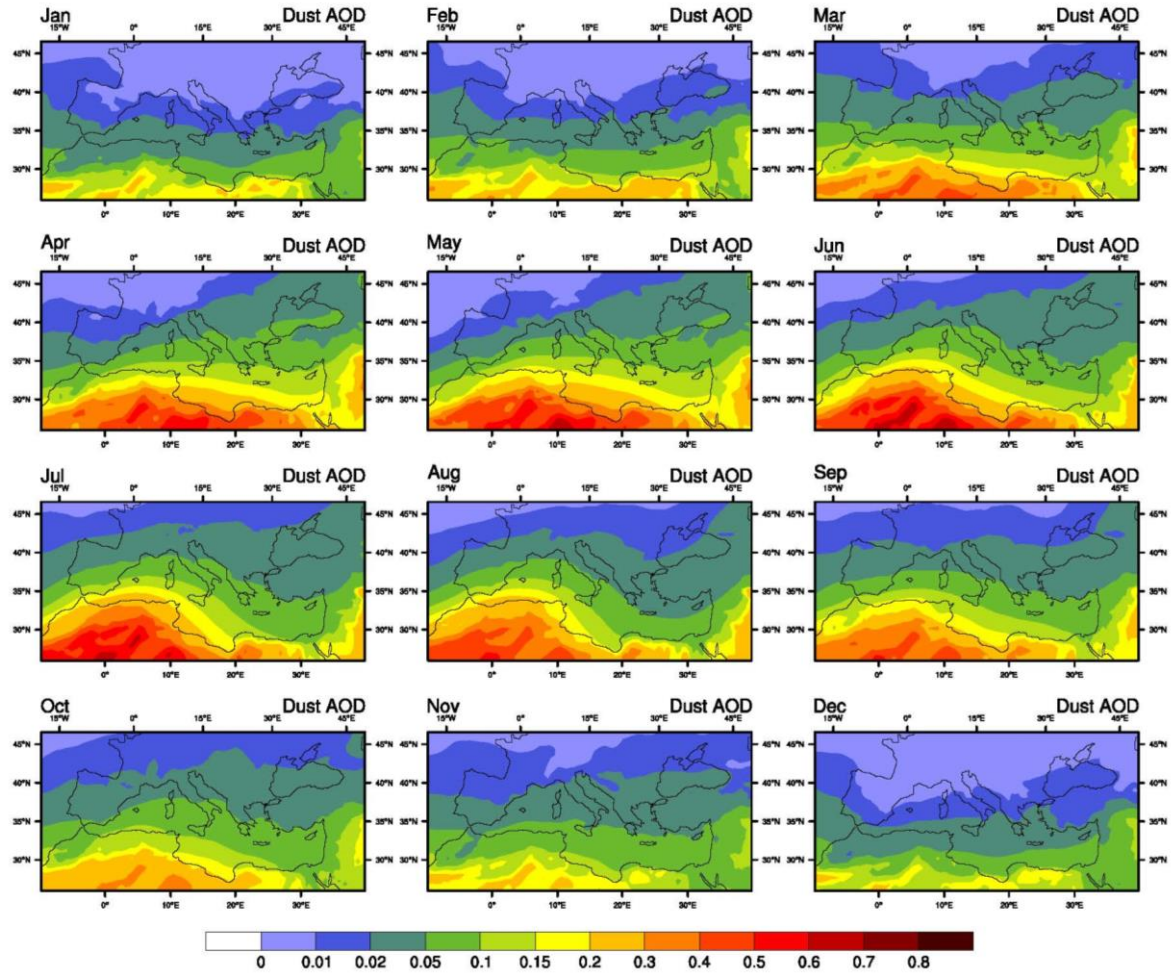

Figure 2. Monthly-averaged dust optical depth at 550 nm (1979-2013 period) over the Mediterranean region from the CNRM-RCSM5 regional coupled climate system model (after Nabat et al., 2015).

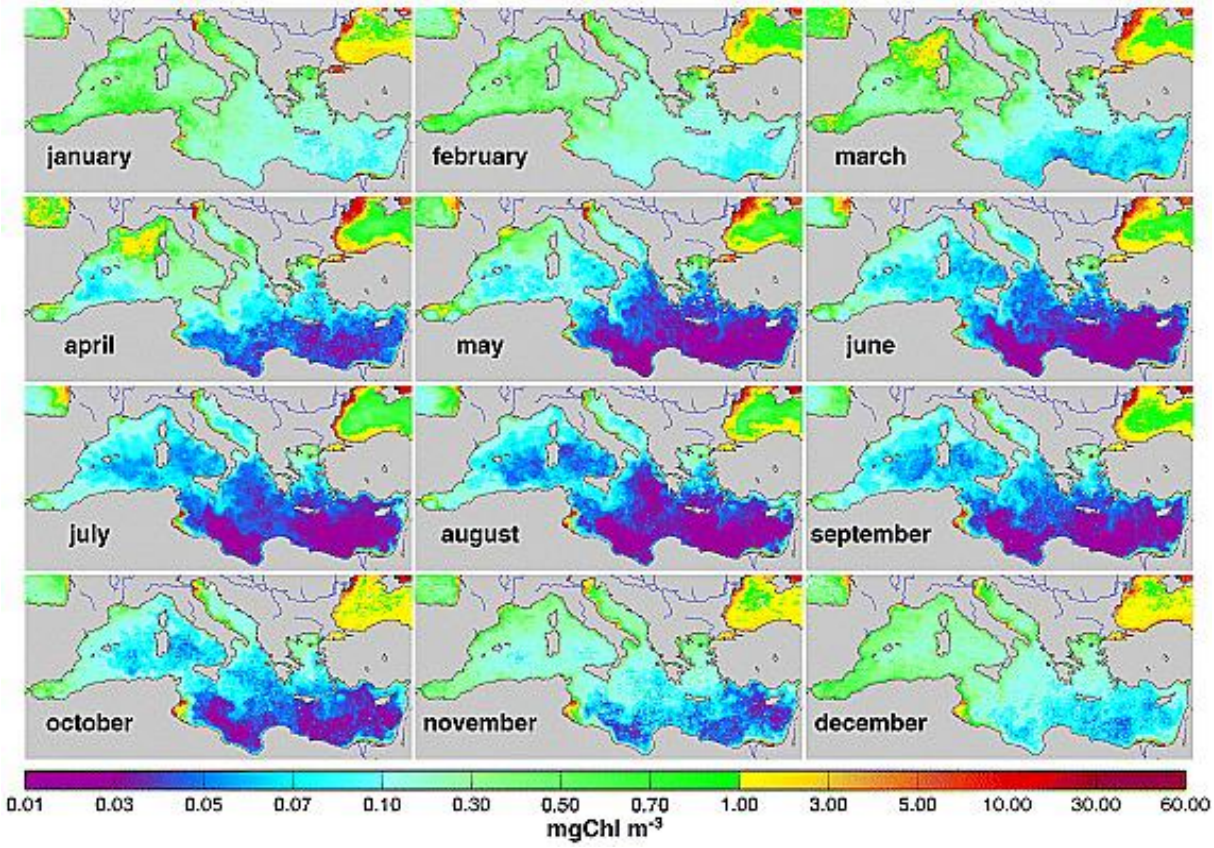

Figure 3. Monthly averaged chlorophyll maps derived from SeaWiFS data for the year 1999 (Bosc et al., 2004; Copyright 2004 by the American Geophysical Union).

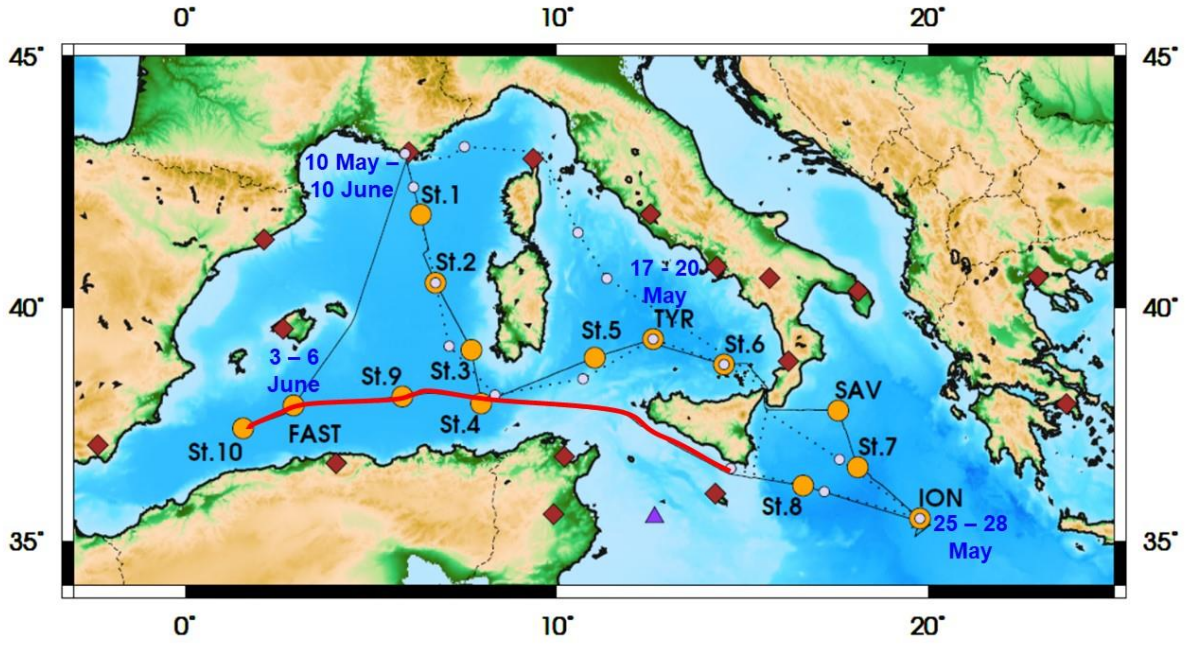

Figure 4. Transect of the PEACETIME Cruise: Initial (dotted line) and final track (continuous line, the red segment corresponds to the change of route to catch a dust

deposition (see section 4); stations are indicated by filled circles (planned stations: smaller, pink: realized: larger, orange). The 10 short stations are numbered from St.1 to St.10. TYR, ION, and FAST indicate the 3 long stations. The SAV station was only performed for the retrieval and launch of floats. The land-based Lampedusa observatory (purple triangle) and 15 AERONET stations (Holben et al., 1998) operated during the cruise provided continuous daytime measurements of the spectral aerosol optical depth (AOD) are also represented (brown diamonds).

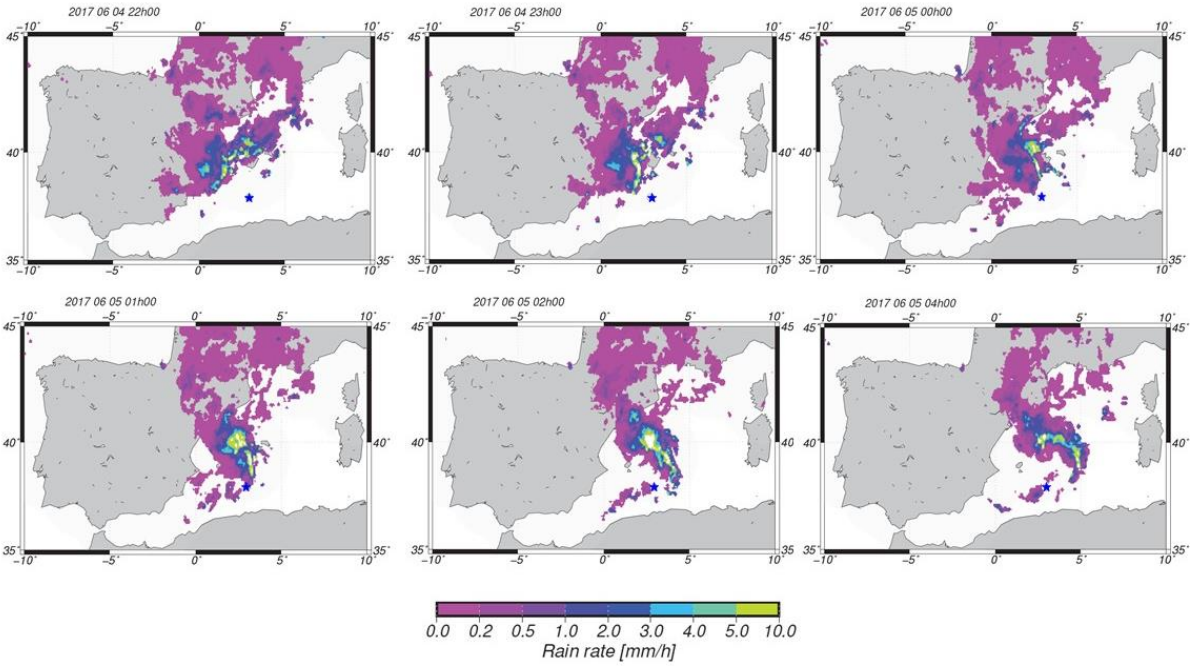

Figure 5. (1) Rain rate (mm h^{-1}) during the night between June 4 and 5 (blue star is the position of the FAST station). These European radar composite products were provided by the Odyssey system, created in the framework of the Opera Program that is the radar component of the Eumetnet observation Program.

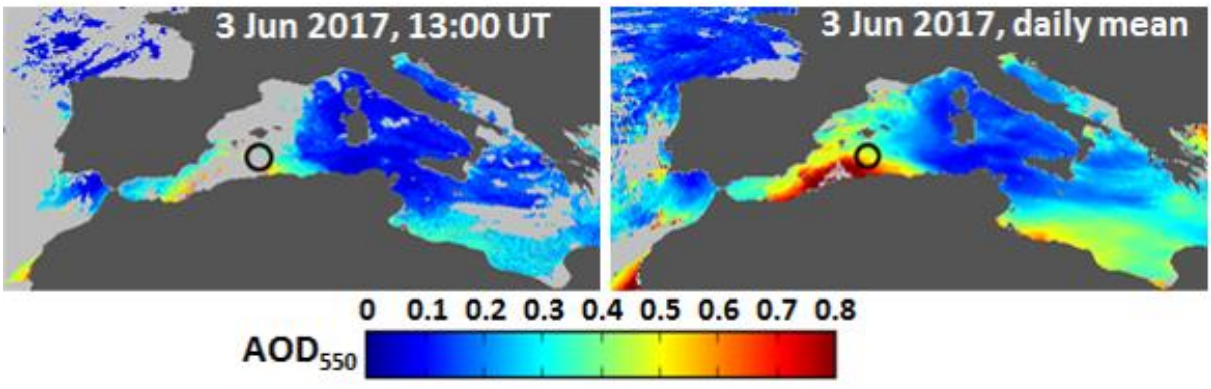

Figure 6. Aerosol optical depth at 550 nm derived from MSG/SEVIRI on 3 June 2017. Left: from the 15-mn image acquired at 13:00 UT. Right: daily average from all 15-min products available between 04:00 and 18:30 UT. The black circle indicates the position of the ship (station FAST). The dark grey mask corresponds to land and coastal ocean pixels, the light grey, to cloudy pixels.

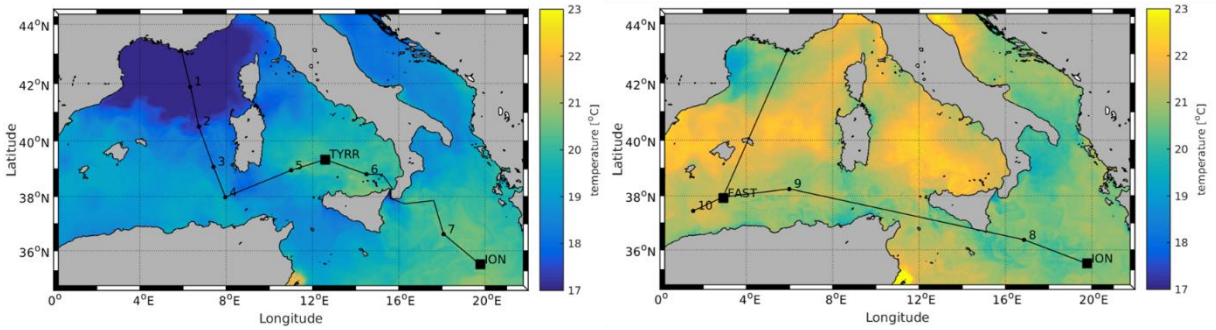

Figure 7. Sea Surface Temperature during the cruise; left) outward route (10-28 May), right) return route (28 May-10 June). The daily satellite pixel data are used to produce a weighted mean. The weight for each pixel is calculated by normalizing by the square of the inverse distance from the pixel to the daily mean ship position. The ship track is shown in black, the short (long) station positions are indicated with black dots (squares). (Courtesy of L. Rousselet).

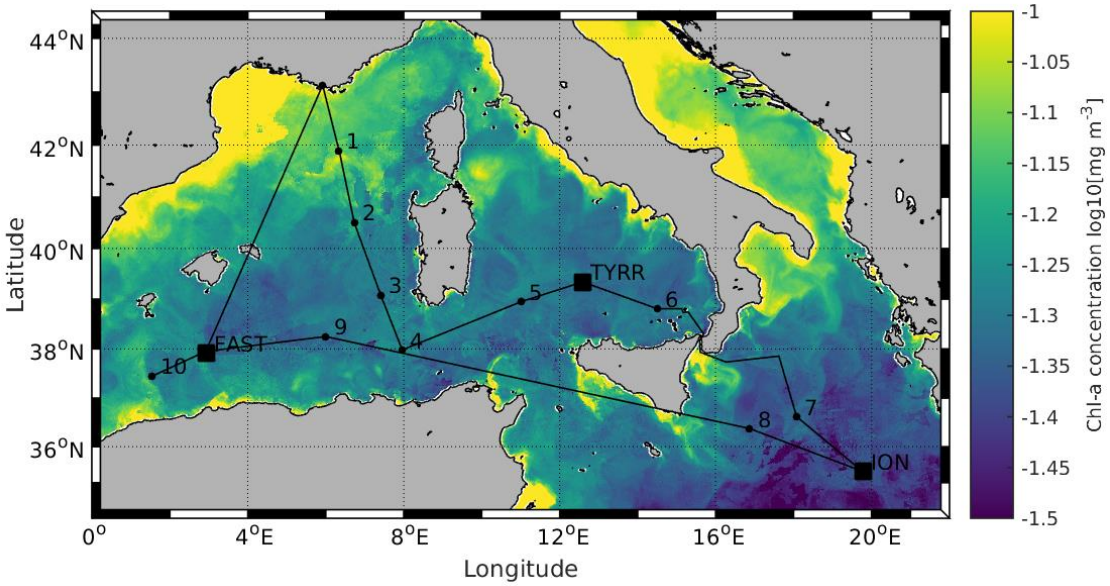

Figure 8. As figure 7, but for the satellite-derived surface Chlorophyll-a concentration averaged over the entire duration of the cruise. (Courtesy of L. Rousselet).

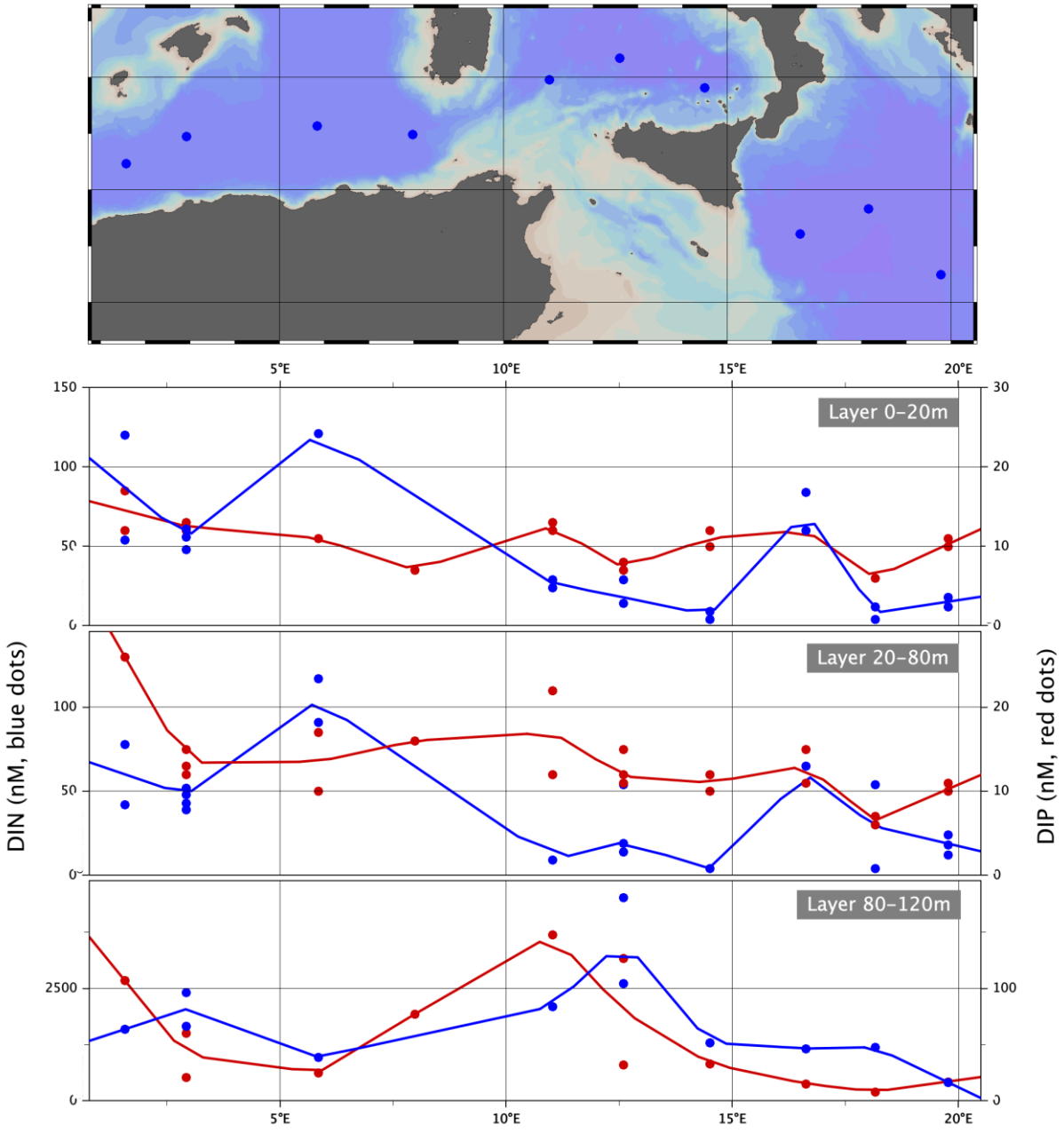

Figure 9. Nitrate (bleu dots) and phosphate (red dots; Pulido-Villena et al., in prep.) concentrations (in nM) in three layers above 120 m, during the PEACETIME cruise along the west-east gradient shown on the map.

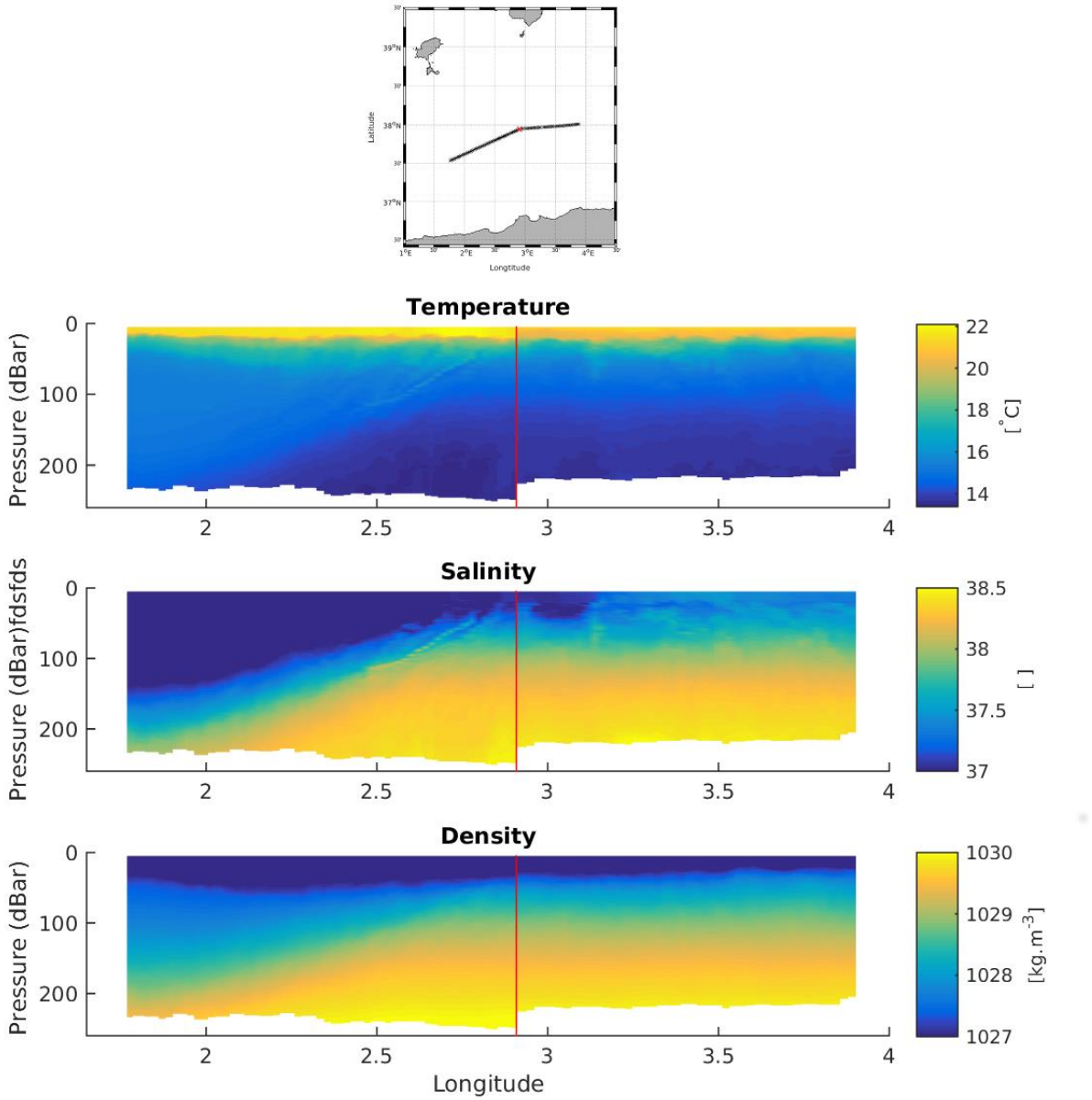

Figure 10. MVP measurements across the FAST station. In the upper panel, the positions of each MVP cast (and of the FAST station) are shown as black (and red) crosses. Below are shown the sections of temperature (top), salinity (middle) and density (bottom).

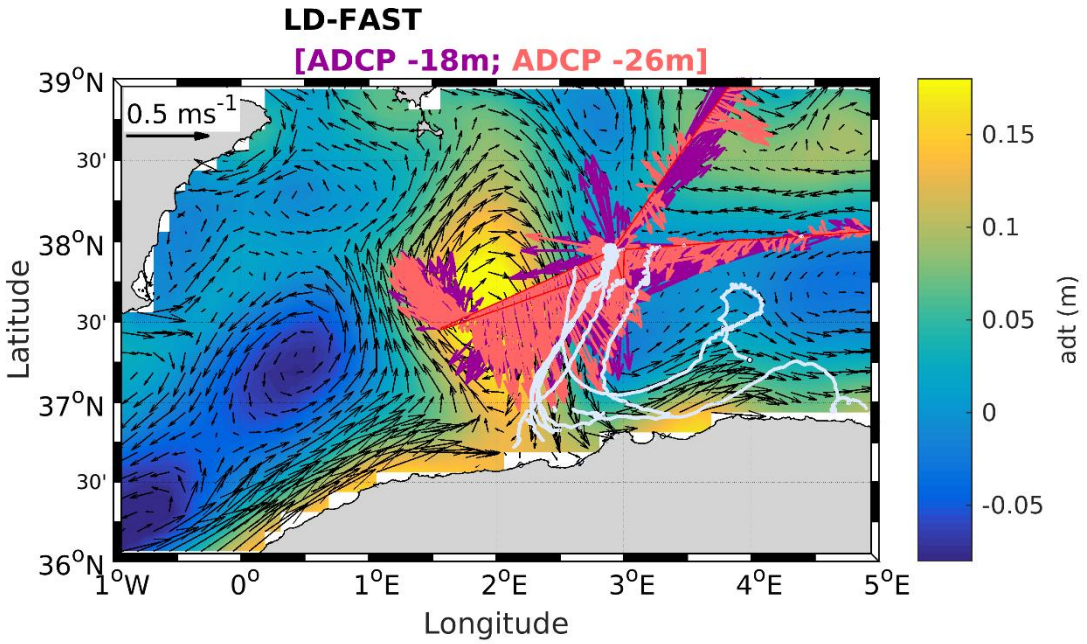

Figure 11. Geostrophic currents from satellite data with the Ekman component from WRF model added (black arrows, mean during the shown transect). In addition, in situ drifter trajectories during 30 days (launched at FAST and in its vicinity) are represented as white lines. Horizontal currents measured by the VM-ADCP for the first two bins (purple arrows -18 m, salmon arrows -26 m) are superimposed for comparison.

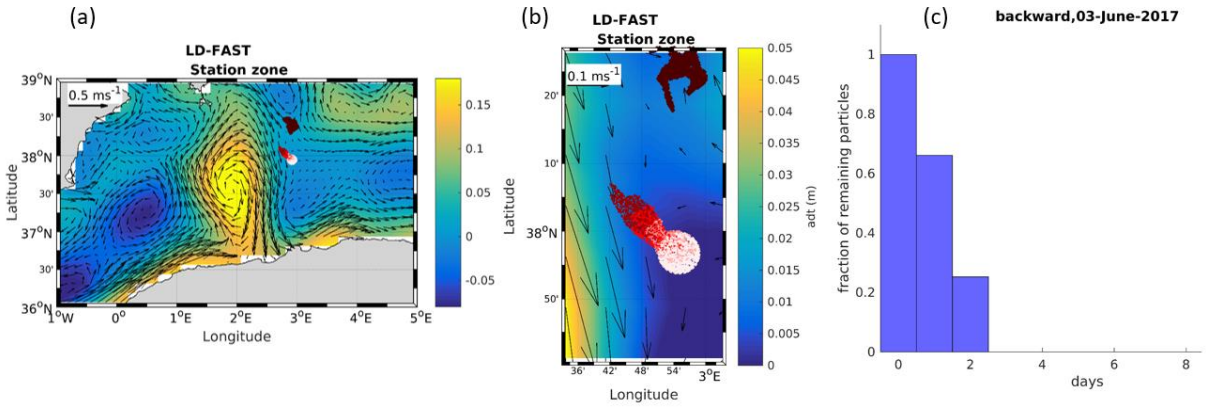

Figure 12. ARIANE particles initial positions (white) and after a backward integration of 1 (pink), 2 (light red), 3 (dark red), and 10 days (black) for the FAST station on the 3rd of June. (a) large view, (b) zoomed view, (c) ratio of particles remaining in the initial zone as a function of the number of backward integration days.

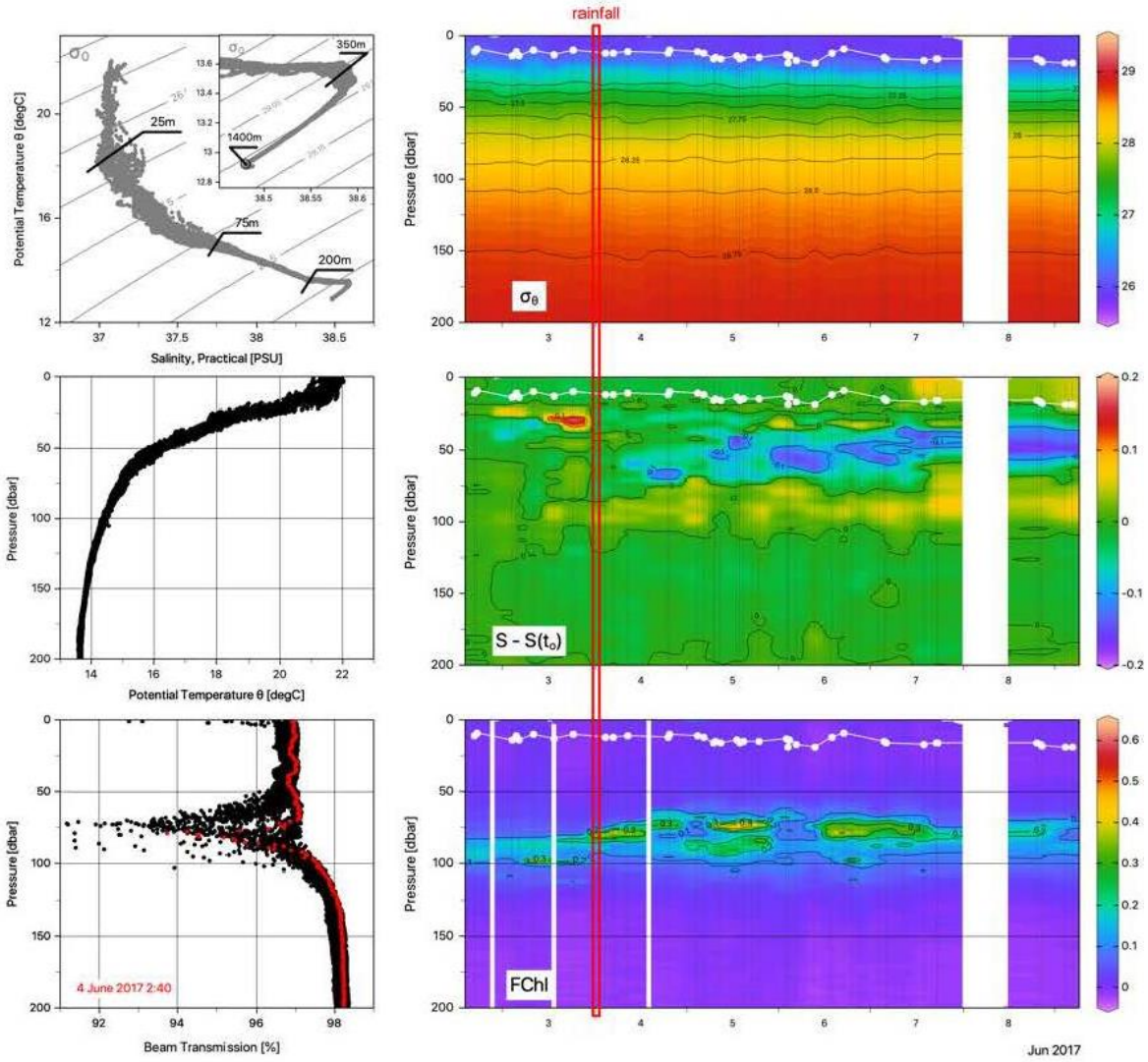

Figure 13. Left panels: temperature-salinity diagram (upper panel), temperature profiles (middle panels), and profiles of beam transmission (lower panel). Right panels: evolution of the surface stratification (sq, upper panel), salinity (anomalies to the profile of June 2, 16h30, middle panel) and chlorophyll fluorescence (lower panel) at the FAST station. Time Series are composed of 43 repeated CTD casts, with variable temporal resolution. The depth of the mixed layer is indicated by white dots. The time of the rainfall is indicated by the red line.